INTERFACE

royalsocietypublishing.org/journal/rsif

Review

Cite this article: Zheng X, Kamat AM, Cao M, Kottapalli AGP. 2021 Creating underwater vision through wavy whiskers: a review of the flow-sensing mechanisms and biomimetic potential of seal whiskers. *J. R. Soc. Interface* **18**: 20210629.
https://doi.org/10.1098/rsif.2021.0629

Received: 3 August 2021
Accepted: 30 September 2021

Subject Category:
Reviews

Subject Areas:
biomimetics, biomechanics

Keywords:
seal whisker, vortex-induced vibration, biomimetics, flow sensing, soft robotics

Author for correspondence:
Amar M. Kamat
e-mail: a.m.kamat@rug.nl

†These authors contributed equally.

Electronic supplementary material is available online at https://doi.org/10.6084/m9.figshare.c.5658543.

THE ROYAL SOCIETY PUBLISHING

Creating underwater vision through wavy whiskers: a review of the flow-sensing mechanisms and biomimetic potential of seal whiskers

Xingwen Zheng[1,†], Amar M. Kamat[1,†], Ming Cao[1] and Ajay Giri Prakash Kottapalli[1,2]

[1]Engineering and Technology Institute Groningen, Faculty of Science and Engineering, University of Groningen, Nijenborgh 4, 9747AG Groningen, The Netherlands
[2]MIT Sea Grant College Program, Massachusetts Institute of Technology, 77 Massachusetts Avenue, Cambridge, MA 02139, USA

XZ, 0000-0003-4993-1896; AMK, 0000-0002-1622-9067; MC, 0000-0001-5472-562X; AGPK, 0000-0002-3868-7069

Seals are known to use their highly sensitive whiskers to precisely follow the hydrodynamic trail left behind by prey. Studies estimate that a seal can track a herring that is swimming as far as 180 m away, indicating an incredible detection apparatus on a par with the echolocation system of dolphins and porpoises. This remarkable sensing capability is enabled by the unique undulating structural morphology of the whisker that suppresses vortex-induced vibrations (VIVs) and thus increases the signal-to-noise ratio of the flow-sensing whiskers. In other words, the whiskers vibrate minimally owing to the seal's swimming motion, eliminating most of the self-induced noise and making them ultrasensitive to the vortices in the wake of escaping prey. Because of this impressive ability, the seal whisker has attracted much attention in the scientific community, encompassing multiple fields of sensory biology, fluid mechanics, biomimetic flow sensing and soft robotics. This article presents a comprehensive review of the seal whisker literature, covering the behavioural experiments on real seals, VIV suppression capabilities enabled by the undulating geometry, wake vortex-sensing mechanisms, morphology and material properties and finally engineering applications inspired by the shape and functionality of seal whiskers. Promising directions for future research are proposed.

1. Introduction

Natural organisms possess well-optimized and specialized systems (e.g. nervous, musculoskeletal and sensory) that are highly adapted to their respective environments owing to millions of years of evolution and natural selection. Sensory systems in the animal kingdom often feature miniaturized biological sensors with high signal-to-noise ratios (SNRs) that filter out unnecessary noise while enhancing useful information from their surroundings [1]. For instance, the sensory organs found in marine animals play a key role in their survival hydrodynamics [2], helping them escape from predators and/or catch prey. Organs such as the lateral line in fishes [3], whiskers in pinnipeds (seals) [4] and dome pressure receptors in crocodiles [5] rely upon the mechanoreception principle to transduce and amplify tiny flow disturbances in their (often murky) surroundings into meaningful signals. The study of the structures, materials, operating principles and functionalities of biological sensors can inspire new ideas for science and technology by serving as ideal models for the optimal design of high-performance biomimetic devices [6].

Pinnipeds are well known for their precise prey-tracking capabilities. They are composed of three families, namely *Otariidae* (fur seals and sea lions), *Odobenidae* (walruses) and *Phocidae* (true or earless seals) [7]. The process of evolution has ensured the gradual adaptation of the pinniped anatomy to its

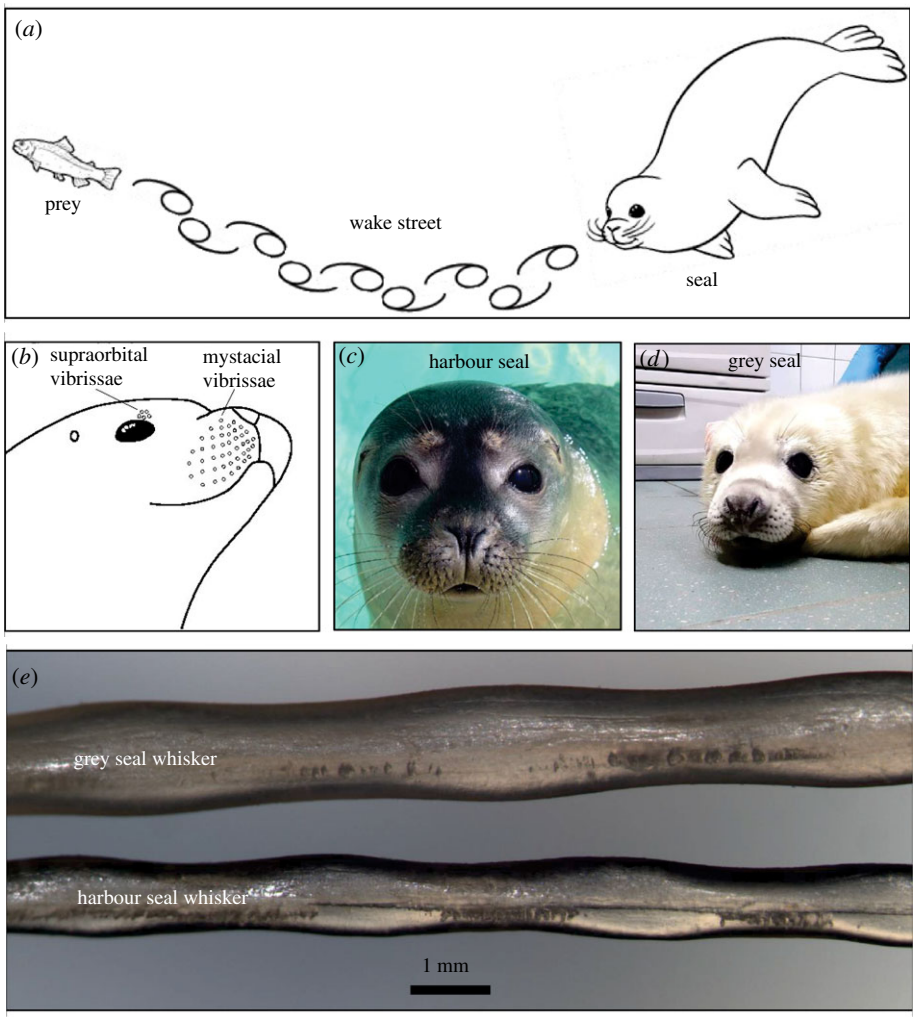

Figure 1. Phocids and their undulating whiskers. (*a*) Schematic of a seal tracking its prey by following the vortices left behind in the wake street. Schematic of seal adapted from ColoringAll.com. Copyright © 2021 ColoringAll.com. (*b*) Arrangement of the array of whiskers on the muzzle of a harbour seal. Adapted from [9]. Copyright © 1995 The Company of Biologists. (*c*) Harbour seal and (*d*) grey seal. Seal photographs courtesy of the Zeehondencentrum (Pieterburen, The Netherlands) and reproduced with permission. (*e*) Optical micrograph showing undulations in grey and harbour seal whiskers along the wider edge of the whiskers.

marine environment. For instance, the body of the pinniped has evolved to be streamlined and sphere-shaped; the former enables it to experience reduced drag forces during swimming [8] while the latter lowers the surface-to-volume ratio of its body to minimize heat loss to the water [7]. However, the aspect of the pinniped anatomy that has attracted the greatest attention in the scientific community is its vibrissae (or whiskers), which function as sensory organs for detecting and interpreting tactile and flow stimuli and are known to play a major role in the pinniped's survival hydrodynamics. The remarkable prey-tracking capability of pinnipeds (illustrated in figure 1*a*) has been partially attributed to the ultrasensitive flow-sensing characteristics of their array of whiskers (figure 1*b* [9]), enabled by the whiskers' high innervation (up to 10× more than found normally in mammals [10]) and unique geometry. In particular, whiskers of pinnipeds belonging to the *Phocidae* family, such as the harbour seal (*Phoca vitulina*, figure 1*c*), grey seal (*Halichoerus grypus*, figure 1*d*), ringed seal (*Pusa hispida*) and spotted seal (*Phoca largha*), exhibit a three-dimensional (3D) 'wavy' geometry (figure 1*e*) that is believed to enhance the SNR of the whisker flow sensors by minimizing vortex-induced vibrations (VIVs). This form–function relationship has obvious implications for biomimetic design, e.g. in flow-sensing applications and vibration-resistant underwater structures, and has thus received considerable attention in the scientific and engineering community in the past decade.

In this first-of-its-kind article, we review the multidisciplinary literature pertaining to the behavioural experiments conducted on real seals, the fluid mechanics of VIV suppression and flow sensing of seal whiskers, the geometric and material properties, and finally engineering applications inspired by the whisker geometry. The paper concludes by suggesting promising directions for future research in this burgeoning field of study. It must be noted that, since the undulating whisker geometry (a focus of the current review) is exhibited only by some seal species from the phocid family, the general term 'seals' will henceforth be used to refer to *Phocidae* unless specified otherwise. The remainder of the paper is organized as follows:

— Section 2 discusses the remarkable prey-tracking capability of seals and provides details on the behavioural experiments conducted on real seals to gauge the whiskers' response against controlled stimuli mimicking fish behaviour.
— Section 3 discusses the effect of the undulating whisker geometry on VIV suppression using insights gleaned from several experimental and numerical studies conducted in the literature, along with proposed whisker–vortex interaction mechanisms.

— Section 4 presents the geometric parameters that characterize undulating seal whiskers, and discusses parametric frameworks used to report the whisker geometry in the literature. Studies reporting the material properties and frequency response of seal whiskers are also discussed.
— Section 5 provides a summary of current and future whisker-inspired engineering applications such as high-SNR flow sensing, drag-reducing turbine blades, oil platform bases in the sea and underwater robots.
— Section 6 summarizes the findings of the review paper and lists some open questions and future directions for research.

2. Behavioural experiments on real seals

2.1. Hydrodynamic trail following

The ability of seals to survive in low-visibility conditions underwater has long intrigued biologists. For instance, it is fascinating to note that blind-yet-healthy seals have been reported in the literature, e.g. on Gertrude Island (Washington state, USA) [11] and in Lake Saimaa (Finland) [10], indicating that seals do not necessarily need to rely upon their sense of vision to hunt for prey. Since seal whiskers were already known to function as sensitive vibrotactile sensors [12], Renouf [13] postulated, as early as 1979, that seals could use their whiskers for hunting fish, since in an incompressible medium such as water (as opposed to air) near-field disturbances could easily generate displacement waves and excite the whiskers (unlike in air); in other words, the whiskers did not need to be in contact with the stimulus to feel its effects underwater. Renouf studied harbour seals hunting for live trout in a controlled environment by changing the values of two variables: the visibility in water (clear or turbid) and the availability of whiskers (i.e. full whiskers or snipped whiskers), leading to a total of four experimental conditions. (It must be noted that such an experiment (namely, snipping of seal whiskers) would not be possible today owing to stricter ethical laws governing behavioural experiments with animals.) Although the seals were able to locate the trout consistently even when their whiskers were cut off, in both clear and turbid water conditions, Renouf [13] observed that the seals with snipped whiskers took longer to catch the trout.

Dehnhardt *et al*. [4] performed the first systematic study of measuring the ability of whiskers to detect minute flow disturbances underwater (figure 2*a*). A harbour seal was trained to indicate (by leaving its station) when it sensed a controlled flow stimulus generated by an oscillating sphere (10–100 Hz) located at an adjustable distance (5–50 cm) away from it underwater. This was a first-of-its-kind experiment, since prior data were only acquired with the whiskers tactilely stimulated in the air [12,16]. The harbour seal responded to very low flow velocities (approx. 245 µm s^{-1} at a stimulating frequency of 50 Hz) even when visual and auditory cues were eliminated. On the other hand, when the seal was fitted with a wire mesh to obstruct its whiskers' motion, it no longer responded to the flow stimuli. Further, it is noteworthy that the displacement, velocity and acceleration sensing thresholds measured for the seal (figure 2*b*) were lower than the corresponding values measured in the wakes of swimming fishes [17], suggesting that the seal whisker sensory system was ideally suited to detecting the flow signatures of fishes and other prey swimming away from them.

Following their initial experiments, Dehnhardt *et al*. [14] conducted another landmark experiment that shed light on the trail-following ability of harbour seals. They used two facts—(i) local flow velocities in the vortex street left behind by a swimming fish persist above the background noise for several minutes after the fish has passed by [17]; and (ii) the seal whisker is sensitive to minute flow velocities that are much lower than the velocities found in the wake of a swimming fish [4]—to arrive at the hypothesis that a seal could use its whiskers to track the trails of fishes several seconds after they had passed by. To verify this hypothesis, Dehnhardt *et al*. [14] trained a harbour seal to track a miniature robotic submarine. The seal displayed a tracking accuracy of around 80% with delay times (i.e. the time difference between the start of the submarine and the start of the seal's search) as long as 20 s. Remarkably, the seal was able to perform these tasks without any visual or auditory cues; however, when the whisker motion was obstructed using a wire mesh, the seal failed to locate the submarine. In the trials, it was critical for the seal to intersect the trail of the submarine to ensure successful tracking; once the whiskers came into contact with the wake of the submarine trail, the seal modified its swimming direction instantly (within 0.5 s [18]) to trace out the exact path and locate the submarine. It must be noted that the seal did not follow the shortest straight-line path to the submarine, but traced the exact trail of the submarine (figure 2*c*). Since the vortices in the wake of a fish are expected to be much more long-lived (approximately several seconds) and stable [17,19] than the turbulent wake of a submarine, it is safe to assume that the seal can perform even better (e.g. with longer delay times) when following a real fish. Although *in vivo* observations of seals tracking real fishes are rare (Renouf [13] reported mostly qualitative data regarding seal behaviour while hunting trout), detection ranges as long as 180 m can be estimated for an exemplar case of a seal tracking herring [14]. Such a long detection range is remarkable for a passive sensing system such as the seal whisker array; to provide context, the estimated detection limits for echolocating mammals such as porpoises and dolphins are reported to be in the range of 70–93 m and 107–173 m [20], respectively.

Schulte-Pelkum *et al*. [15] improved upon the experiment of Dehnhardt *et al*. [14] by generating a more natural hydrodynamic trail using a harbour seal (as opposed to an artificial trail using a miniature submarine) and training a second harbour seal to follow the biogenic trail generated by the first. The trail was well characterized using particle image velocimetry (PIV) measurements and local velocities of around 30 mm s^{-1} in the wake were recorded 30 s after the first seal had swum by. Again, although both visual and acoustic cues were eliminated, the seal displayed impressive success rates of 80–90% in following the trail. Interestingly, two strategies were adopted by the seal: in around 63% of the successful trials, the seal followed the trail linearly, while in 34% of the successful trials, the seal followed a zigzag trajectory, intersecting the trail multiple times and evidently using a self-correcting mechanism to not stray away from the trail (figure 2*d*). The seminal behavioural experiments of Dehnhardt *et al*. [4,14] and Schulte-Pelkum *et al*. [15] proved, for the first time, that seal whiskers could serve as ultrasensitive flow sensors (in addition to being vibrotactile sensors) that could aid or even substitute for the sense of vision when executing survival hydrodynamics.

2.2. Response to controlled stimuli

Following the work of Dehnhardt *et al*. [4,14], many experiments (mostly performed by Dehnhardt and colleagues at

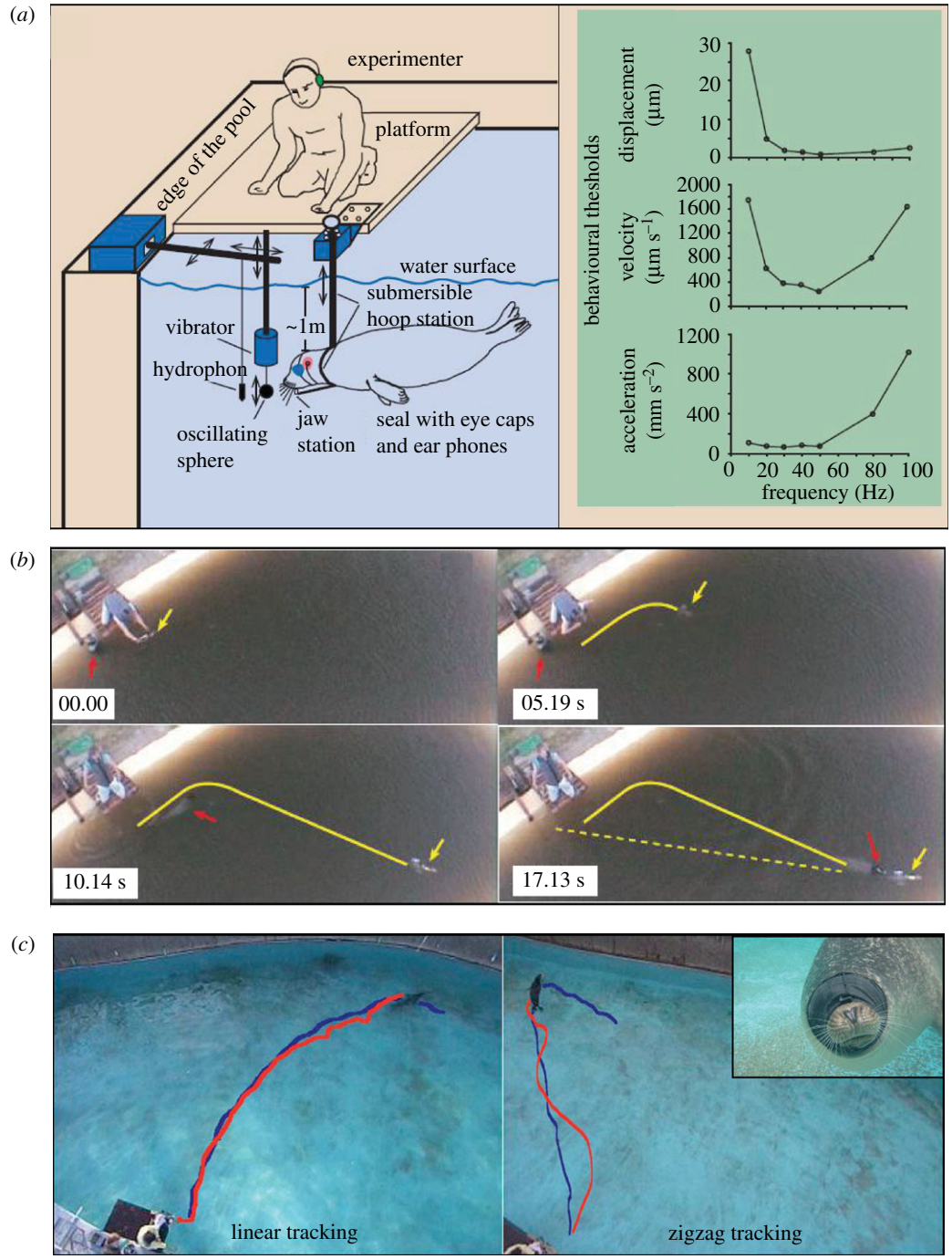

Figure 2. Hydrodynamic sensitivity and trail-following experiments with real seals. (*a*) Experimental set-up to determine sensing thresholds of harbour seals to a controlled oscillatory stimulus. Adapted from [4]. Copyright © 1998 Springer Nature. Reprinted with permission. (*b*) Blindfolded harbour seal tracking the exact path of a submarine with a 10 s delay. Yellow arrow: submarine; red arrow: harbour seal; yellow solid line: trail of submarine (followed by the seal); yellow dotted line: straight-line path to submarine (not followed by the seal). Adapted from [14]. Copyright © 2001 AAAS. Reprinted with permission. (*c*) Two tracking strategies, namely linear (left) and zigzag (right), adopted by the blindfolded seal (inset) while following a biogenic trail. Blue denotes the biogenic trail generated by the first seal, and red denotes the path of the second (following) seal. Adapted from [15]. Copyright © 2007 The Company of Biologists. Auditory and visual cues were eliminated in all the above experiments.

the University of Rostock, Germany) were subsequently conducted with harbour seals to understand their response to controlled stimuli that mimicked fish behaviour. Wieskotten *et al*. [18,21] conducted psychophysical experiments demonstrating the ability of a blindfolded harbour seal to correctly determine the direction, size and shape of objects towed in front of it (figure 3*a*). PIV measurements indicated that the wake behind the towed objects contained counter-rotating vortices with a laminar jet between them that contained the highest flow velocities (an exemplar flow field containing such features [22] is shown in figure 3*b*). Once the seal whiskers came into contact with the vortices (figure 3*c*), the seal took very little time (approx. 0.5 s) to determine the direction of the towed object. The flow fields shown in figure 3*b*,*c* are similar in their basic structure to the reverse Kármán streets ('reverse' because the signs of vortices are opposite to those expected in a normal Kármán street [23]) typically present in the wake of fishes (figure 3*d*). Wieskotten *et al*. [21] correlated the response of the seal to the flow fields generated in the wake of differently sized and shaped objects (figure 3*a*),

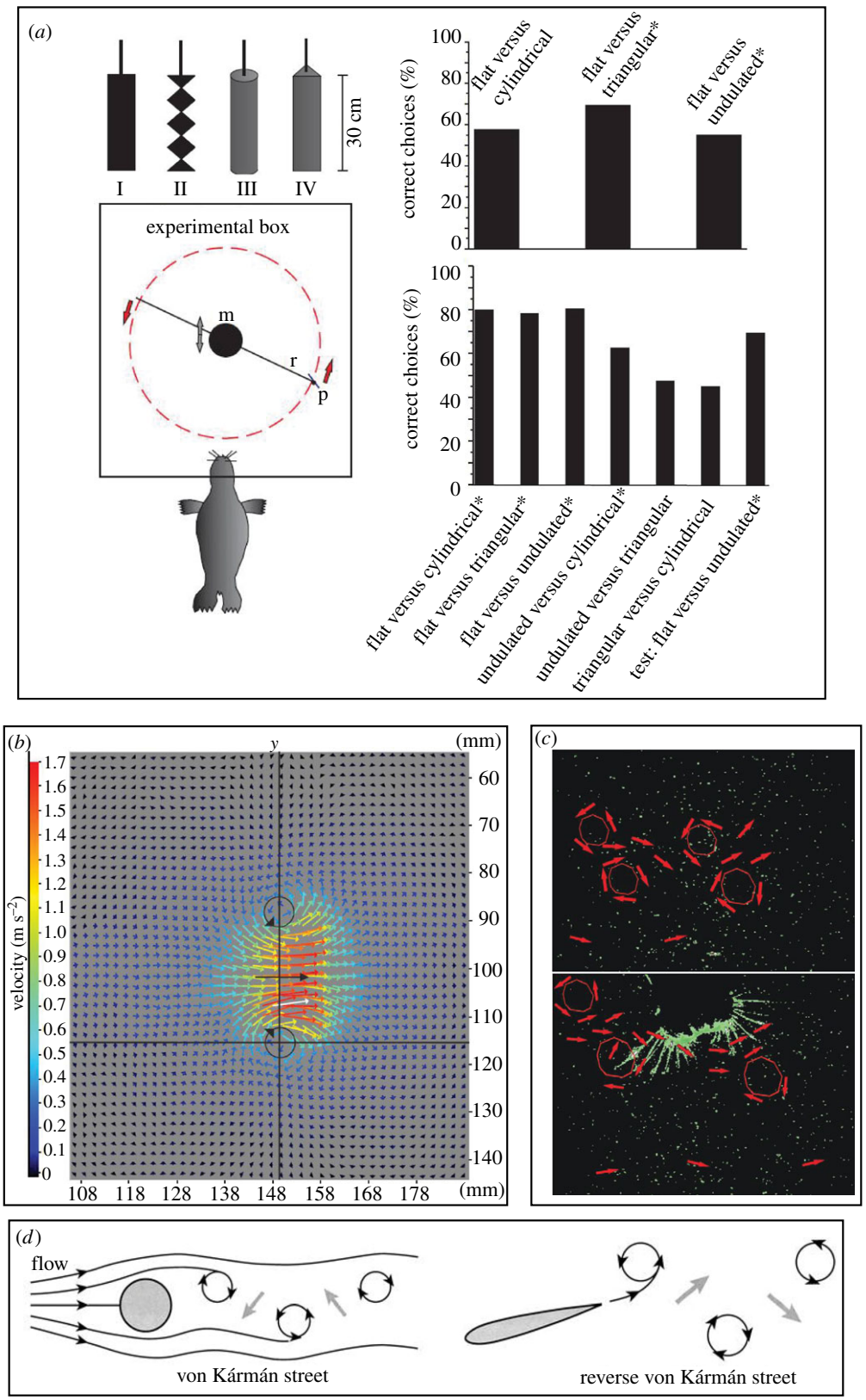

Figure 3. The response of harbour seals to controlled stimuli. (*a*) Experimental set-up to determine the response to objects of different sizes and shapes towed before the seal (m, motor; r, rotor system; p, paddle), and the ability of the seal to distinguish between different object sizes/shapes. Asterisks indicate a significant ability to differentiate between the two shapes. Adapted from [21]. Copyright © 2011 The Company of Biologists. (*b*) A flow field (generated here using a vortex ring generator) that is typically associated with the wake of towed objects, consisting of a pair of counter-rotating vortices with a laminar jet between them that contains the highest flow velocities. Adapted from [22]. Copyright © 2018 The Company of Biologists. (*c*) PIV snapshots of the wake of an artificial fin (not shown) towed in water, containing pairs of counter-rotating vortices (top) and the interaction of the seal's protracted whiskers with the wake vortices (bottom). Red arrows indicate flow velocities and red circles indicate vortex rings. Adapted from [18]. Copyright © 2010, The Company of Biologists. (*d*) Schematic of regular and reverse Kármán vortex streets comprising counter-rotating vortices (black circles with arrows) and a central laminar jet flow (grey arrows). Adapted from [23]. Copyright © 2002 Oxford University Press. Reprinted with permission.

and reasoned that counter-rotating vortices within the trail could be a significant marker that is used by seals to extract information from the trail. Recent studies have shown that the harbour seal is indeed sensitive to single vortex rings [22]. The exquisite sensitivity of seals to benthic fish-like breathing was also demonstrated by Niesterok *et al*. [24] by

using underwater nozzles to mimic the breathing currents. The experiments [24] proved that, in addition to counter-rotating vortices [21], seal whiskers could also be sensitive to vortex-free jet flows such as those generated by benthic fish breathing, indicating the versatility of the whisker sensory system. The comprehensive studies of Wieskotten *et al*. [18,21] demonstrated that seals could interpret the information encoded within a given hydrodynamic trail to know not only the direction but also the size of escaping prey such as fish, an ability that could be used to make decisions regarding whether to embark upon an energy-consuming hunt or not depending upon the calorie reward offered by the (small or large) fish.

Apart from the group at the University of Rostock, behavioural experiments on real seals were also performed at the University of California (Santa Cruz). Murphy *et al*. [25] subjected a harbour seal (again, eliminating any visual or auditory cues) to oscillatory stimuli. The experiments were similar to the ones conducted by Dehnhardt *et al*. [4] (§2.1), with two main differences: (i) the seal was excited using a vibrating plate that was directly in contact with the whiskers in the air (as opposed to oscillatory excitation underwater from a distance [4]); and (ii) the excitation was conducted over a much broader frequency range (10–1000 Hz) than in Dehnhardt *et al*.'s [4] work. Although the stimuli applied by Murphy *et al*. [25] in their psychophysical experiments may be classified as vibrotactile rather than flow in nature (the latter being the focus of this review article), the results were still instructive since they demonstrated the ability of the seal whiskers to respond to higher frequencies (i.e. greater than 100 Hz) that are common for hydrodynamic stimuli. Moreover, since the whiskers were stimulated via direct contact, the exact displacement, velocity and acceleration of the stimulus at the whisker were known, unlike earlier work [4] where these respective values near the whisker had to be estimated using potential flow theory. The lowest velocity-sensing thresholds (i.e. highest sensitivity to velocity) were found to be in the range of 20–250 Hz, with the best sensitivity (corresponding to the lowest displacement, velocity or acceleration thresholds) observed around 80 Hz. Since most hydrodynamic stimuli of relevance to seals are expected to lie within this range (e.g. frequencies in the wake of swimming fishes often exceed 100 Hz [17]), this tuning seems reasonable. It must be noted that which hydrodynamic variable is of most importance to the seals with respect to flow sensing is still an open question and deserves further attention. Unlike the fish lateral line system that is fairly well understood in terms of its operating mechanisms—the superficial neuromasts are velocity sensors that are sensitive to low-frequency stimuli (e.g. the fish's own swimming motion and water currents) while the canal neuromasts act as acceleration sensors that are attuned to higher frequencies corresponding to flow disturbances (e.g. caused by prey or predators nearby) [26]—the seal whisker system has not reached this level of maturity in terms of our understanding. This may be attributed in part to the difficulties in performing electrophysiological studies on seals to record afferent fibre outputs as a function of flow stimuli (only one such dataset from 1975 [27] exists for grey and harbour seals), as is common in the fish lateral line literature.

In spite of the limitations mentioned above, some insights can still be gleaned from the behavioural experiments. For instance, the PIV measurements [18,21] indicated that the counter-rotating vortices with a central jet flow (figure 3*b*) are important elements of a flow wake that the seal could use to determine both the direction and size of the moving object generating the flow pattern. More recent experiments [22,24] proved that the seal can gauge the direction of a single vortical ring and is able to locate pulsed breathing currents. Since vortical flow fields and pulsed breathing currents both comprise high-velocity gradients, these results seem to indicate that flow acceleration could be a more crucial sensory cue (compared with displacement and velocity) to the seal whisker system, at least from the point of view of trail following and hunting for prey. Such a conclusion is also supported by the acceleration tuning curves of Dehnhardt *et al*. [4] (figure 2*a*, right) and Murphy *et al*. [25], who observed low acceleration thresholds (and hence high sensitivity to flow acceleration) in the frequency range of relevant hydrodynamic events (less than 80 Hz [4] and less than 250 Hz [25], respectively). However, since velocity is a more intuitive metric that is generally used to characterize flow sensors, it is customary to report velocity-sensing thresholds in the literature, e.g. 0.245 mm s^{-1} at 50 Hz [4] and 0.09 mm s^{-1} at 80 Hz [25] (note that these are oscillatory velocities represented as root mean squares at the respective frequencies, and hence have an acceleration component necessarily associated with them). Table 1 presents a summary of the behavioural experiments discussed above.

3. Seal whisker as a flow sensor

3.1. Role of undulating morphology

The findings reviewed in §2 clearly demonstrate the central role played by seal whiskers in flow sensing, with reported sensitivities to (oscillatory) flow velocities of less than 1 mm s^{-1} [4]. Considering the fact that harbour seals are known to swim at speeds of around 0.5–2 m s^{-1} while foraging [28], this represents an impressive feat of being sensitive to velocities of up to 500–2000× lower than the seal's swimming speed. The exquisite sensitivity of seal whiskers to minute hydrodynamic stimuli may be attributed to their highly adapted follicle–sinus complex (FSC), which houses up to 10× times more nerve fibres than terrestrial mammals [10]. While an in-depth discussion of the innervation patterns of seal whiskers is outside the scope of the present article, the reader is referred to publications that studied the FSC microstructure of various seal species in great detail (e.g. in bearded seals [29], northern elephant seals [30] and harbour seals [31]) and discussed the consequences of a highly innervated FSC for the enhanced foraging abilities of seals.

In addition to the high innervation, there is also a geometric factor at play that is responsible for the trail-tracking ability of seals. Moving objects become unstable at high speeds, especially underwater. When a high-aspect-ratio bluff body is placed in a water flow (or, alternatively, is towed in still water), it experiences vibrations in the cross-flow direction. The vibrations are attributed to flow instabilities that occur in the wake as a result of flow separation from the sharply curved edges of the bluff body. Such flow instabilities cause staggered vortices of alternating signs to be shed from either side of the object, giving rise to a Kármán vortex street in the wake of the object (an example can be seen in figure 3*d*, left). Such vortex shedding loads the body transversely in an alternate and periodic manner from both sides. If the natural frequency of the structure is

Table 1. Behavioural experiments on live seals.

Renouf [13]	
main investigation:	Observations of harbour seals (with intact or snipped whiskers in turbid or clear water) hunting live trout.
main result:	Harbour seals took longer to catch trout when their whiskers were snipped.
Dehnhardt *et al*. [4]	
main investigation:	Sensitivity of seal whiskers to controlled oscillatory stimuli applied underwater at a distance.
main result:	Flow-sensing thresholds as low as 245 µm s^{-1} (at 50 Hz) were observed.
Dehnhardt *et al*. [14]	
main investigation:	Hydrodynamic trail-following ability of harbour seals.
main result:	Harbour seals could track a robotic submarine using only their whiskers.
Schulte-Pelkum *et al*. [15]	
main investigation:	Hydrodynamic (biogenic) trail-following ability of harbour seals.
main result:	Harbour seals used two (linear and zigzag) tracking strategies while following a biogenic trail.
Wieskotten *et al*. [18,21]	
main investigation:	Sensitivity to wakes generated by objects of different sizes and shapes.
main result:	Harbour seal could identify the direction of towing and distinguish between the sizes and shapes of objects.
Murphy *et al*. [25]	
main investigation:	Sensitivity to controlled oscillatory stimuli applied by direct contact.
main result:	Frequency range of the highest sensitivity found to be approximately 20–250 Hz.
Niesterok *et al*. [24]	
main investigation:	Sensitivity of seals to artificial benthic fish-like breathing currents.
main result:	Harbour seal is sensitive to benthic fish breathing and can sense vortex-free jet flows.
Krüger *et al*. [22]	
main investigation:	Sensitivity of seals to single vortex rings.
main result:	Harbour seal can detect the direction of a single vortex ring irrespective of the direction of impact with the whisker.

excited by this periodic loading and the damping is low enough, the structure can experience significant oscillations, resulting in VIVs. It is obvious that, for a structure such as the seal whisker to act as an underwater sensor, VIVs represent undesirable noise that could potentially interfere with the signal from the hydrodynamic trail that it wishes to sense. A simple algebraic exercise can demonstrate this point. Consider a seal swimming at a typical velocity of $U_\infty = 0.5\ \mathrm{m\ s^{-1}}$ [32]. Assuming the characteristic dimension D of its whisker to be 1 mm [33] and the Strouhal number (St) to be 0.21 [34], we can estimate the frequency of vortex shedding (and hence of VIVs) to be $f_{\mathrm{VIV}} \sim 100$ Hz using the definition of St [34],

$$f_{\mathrm{VIV}} = \frac{St \times U_\infty}{D}. \tag{3.1}$$

This VIV frequency of approximately 100 Hz falls well within the frequency range of sensitivity measured for harbour seals [4,16,25] (figure 2*a*) and can also, more importantly, interfere with relevant hydrodynamic frequencies (at least 100 Hz [17]) associated with the wakes of escaping prey. Hence, suppression of such VIV-generated noise must be central to the seal whisker's exemplary flow-sensing ability.

It is well known in the fluid mechanics literature that geometric modifications can significantly change the vortex-shedding behaviour in the wake of a structure, a strategy that is known as 'passive control' since it does not require any power input to achieve its aims [35]. Such modifications take the form of surface protrusions (e.g. helical strakes), shrouds (e.g. perforations) or near-wake stabilizers (e.g. guiding vanes), and can reduce VIVs by displacing the vortex formation region further downstream and thus away from the structure [36]. Introducing 'waviness' into a cylinder is also known to reduce both drag and lift coefficients [37,38]. The whiskers of phocid seals possess a unique morphology that is distinct from most mammalian whiskers, including seals from the otariid and odobenid families. Harbour seals, for instance, possess whiskers that are approximately elliptical (or 'flattened') in cross-section with periodic variation in both the major and minor axes of the ellipse along the whisker length; such a morphology has been described as 'undulating' [39], 'wavy' [32], 'beaded' [40] or 'lobulated' [41] in the literature (the first two terms will be used interchangeably in this article). This undulating morphology has been noted by biologists since at least the 1960s [41]; however, its evolutionary benefits towards the whisker's function were largely unexplored until around 2010 [32].

Combining the fluid mechanical insights discussed above and their own measurements of flow-sensing thresholds of harbour seals, Hanke *et al*. [32] postulated that the undulating whisker geometry could suppress VIVs when the seal swims. Using a series of experimental and numerical techniques that included mounting a camera on a harbour seal to observe the whisker vibrations during hydrodynamic trail following, comparing the vibrations of (excised) isolated whiskers

belonging to a harbour seal (undulating) and a California sea lion (no undulations) using a piezoelectric transducer and computational fluid dynamics (CFD) simulations, and finally using micro-PIV techniques to compare the flow field in the wake of an excised harbour seal whisker, Hanke *et al*. [32] showed that the harbour seal whisker demonstrated a VIV response that was up to 6× lower than that of the California sea lion whisker. Since the Reynolds number (*Re*) was similar for the two experiments, the difference in VIV response could only arise from the undulating geometry of the harbour seal whisker. Using a combination of PIV and CFD results, three major reasons for the lower VIV response were identified (figure 4*a*, left [32]): (i) the undulating whisker structure was able to disrupt the coherence of the organized street of alternating sign vortex tubes (Kármán street) that would otherwise exist in the wake of a smoother structure (e.g. figure 3*d*, left); (ii) the vortex formation was delayed, thus pushing the flow instabilities further downstream and away from the whisker; and finally (iii) the undulating whisker shape made the pressure field more symmetric than a corresponding cylindrical shape. The disruption of the vortex coherence due to the undulating whisker geometry was also observed in later experiments conducted using dye visualization (figure 4*a*, right [39]). The resulting incoherent wake behind the whisker decreased the time-dependent lift coefficient (and hence VIVs), as shown in figure 4*b* [32]. Video recordings of the harbour seal whiskers did not reveal any discernable whisker vibration during trail following (swim speeds approx. 0.5–1 m s^{-1}), further supporting the claim of VIV suppression. Although the last result may well be due to frame rate and resolution limitations of the camera (the frames per second or 'fps' of the recording was not specified in the paper and the spatial resolution was 0.2 mm), the findings were exciting not only from the point of view of sensory biologists but also fluid dynamicists and engineers who could take inspiration from the seal whisker's undulating geometry as a potential paradigm for designing VIV-resistant structures exposed to flow.

Following the work of Hanke *et al*. [32], subsequent studies were conducted (both experimental and computational) to better understand the fluid–structure interactions when an undulating whisker was placed in water flow. Owing to limited access to real seal whiskers and the technical challenges of performing vibration and fluid-flow measurements at the small scale of the seal whisker (cross-sectional dimensions less than 1 mm), several researchers also used approaches such as physical modelling (e.g. by performing experiments on scaled-up whisker-like structures [39,44–46]) and numerical modelling [47–50] to study the effect of undulations on VIVs. The discussion that follows in this subsection will focus mainly on work performed on real seal whiskers.

Miersch *et al*. [42] extended the work of Hanke *et al*. [32] by subjecting isolated harbour seal and California sea lion whiskers (embedded in a piezoelectric transducer) to water flow while also exciting them using an upstream cylinder that shed vortices periodically (frequency = f_{VS}) and predictably; in other words, the whiskers were placed in a controlled Kármán vortex street. Such a vortex generator served as an approximation to the fish wake (figure 3*d*) that the whiskers would be expected to encounter in a real-life scenario. In these experiments, f_{VS} was the signal to be sensed and the VIV was the noise experienced by both whiskers due to their own vortex shedding. Comparing the piezoelectric output from both whiskers and converting the time-series data into the frequency domain (to check if the whisker-on-sensor system showed a dominant peak at f_{VS}), Miersch *et al*. [42] showed that the undulating harbour seal whisker demonstrated a much higher SNR than the smoother California seal whisker owing to a 10× reduction in VIV (figure 4*c*). More recently, Bunjevac *et al*. [43] experimentally studied the downstream wake region of an undulating elephant seal whisker and compared it with that generated by a smooth California sea lion whisker. Unlike previous work [32] that only studied 15 mm of the whisker length, Bunjevac *et al*. [43] observed the wake behind the full whiskers using PIV (figure 4*d*), a challenging task given the natural curvature of the whiskers, and found that the undulations significantly reduced the reversed flow region behind the whisker, indicating reduced vorticity. Further, the undulations were also responsible for reducing the magnitude of turbulent intensity (figure 4*d*) by promoting mixing within the wake. The flow-instability regions were seen to be pushed further downstream, agreeing with previous work [32].

On the other hand, in their comparative study on the in-flow behaviour of an isolated harbour seal whisker, elephant seal whisker and a California sea lion whisker, Murphy *et al*. [33] observed no differences in the VIV response of the whiskers. This result was surprising since it is the only study of its kind to have found a lack of correlation between the undulating whisker surface and VIV suppression. Experiments conducted with scaled-up (20×) plastic models of harbour seal whiskers [39] also demonstrated that undulations played a key role in reducing VIVs. It must be pointed out that Murphy *et al*. [33] measured the velocity of vibrations at the midpoint of the respective whiskers (using laser vibrometry) to compare the VIV responses of the three whiskers, as opposed to other approaches [32,39,42], where the bending forces at the whisker base were correlated with VIVs. Because of the greater cross-sectional area of the smoother sea lion whisker compared with the 'flattened' undulating harbour and elephant seal whiskers [33], the midpoint of the sea lion whisker (where the measurement was conducted) might have vibrated at a lower velocity owing to its higher bending stiffness. Moreover, the tested sea lion whiskers were also shorter (approx. 60 mm) than the other two species (approx. 70 mm) [33], which could have caused lower velocities at the whisker's midpoint. Nonetheless, we note that more tests with real seal whiskers are necessary to resolve this discrepancy in the literature. A summary of the results discussed above is provided in table 2, while an extended summary can be found in electronic supplementary material, table S1, Sheet 1 and is also available publicly as a GitHub repository (https://github.com/ZhengXingwen/Flow-sensing-mechanisms-and-biomimetic-potential-of-seal-whiskers.git).

The role played by undulations in the seal whisker is undoubtedly important for the seal's foraging activities. It may be argued, however, that the whisker's wavy geometry is not critical for hydrodynamic trail following, since many seal species, especially those belonging to the otariid and odobenid families, do not display such a wavy geometry and are yet perfectly capable of hunting for prey. Behavioural experiments conducted with California sea lions [51] (similar to the hydrodynamic trail-following experiments on harbour seals [14] described in §2.1) demonstrated that the blindfolded sea lions were able to follow the trail at a comparable success rate to that of the harbour seal. However, it was found that the success rates decreased when: (i) the delay time between the submarine passing and the start of

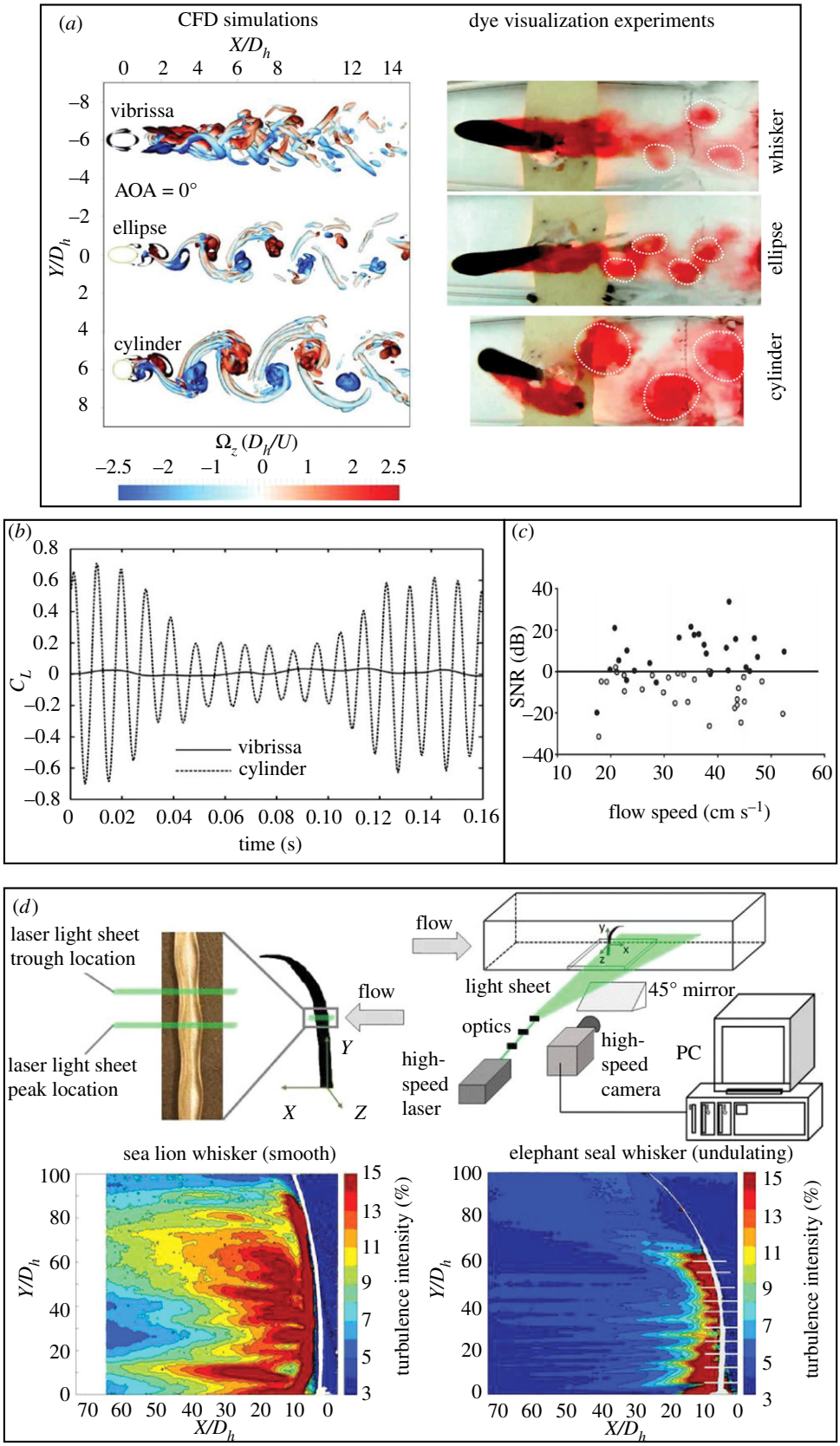

Figure 4. Effect of undulations on VIVs. (*a*) CFD simulations (left) showing the vorticity in the wake of a circular cylinder, an elliptical cylinder and a harbour seal whisker model. Adapted from [32]. Copyright © 2010 The Company of Biologists. Dye visualization experiments (right) showing the incoherent vortices in the wake behind an undulating whisker-like structure compared with the circular and elliptical cylinders. Adapted from [39]. Copyright © 2015 Cambridge University Press. Reprinted with permission. The whisker-like undulating model is seen to disrupt the coherence of the Kármán vortex street and displaces the vortex formation region further downstream compared with the two cylinders. (*b*) Evolution of the lift coefficient (which is directly related to VIVs), C_L, as a function of time, calculated for the circular cylinder and the seal whisker model, indicating 90% reduction in VIV response for the whisker. Adapted from [32]. Copyright © 2010 The Company of Biologists. (*c*) SNR measured for excised harbour seal (black dots) and California sea lion (grey dots) whisker segments in steady water flow with an upstream vortex generator as the signal, showing the significant elimination of VIV-related noise in the former. Adapted from [42]. Copyright © 2011 The Royal Society. Reprinted with permission. (*d*) PIV measurements for excised elephant seal and California sea lion whiskers, conducted for the entire whisker length, showing the vastly reduced turbulent zone (in both intensity and size) behind the undulating elephant seal whisker. Adapted from [43]. Copyright © 2011 Springer Nature. Reprinted with permission.

Table 2. Effect of whisker undulations on VIVs.

Hanke *et al*. [32]	
techniques:	Head-mounted video recordings, force measurement at the base of excised whiskers using piezoelectric transducer, micro-PIV, CFD simulations.
findings:	Undulations reduced the primary vortex separation region, displaced the first vortices further downstream and made the pressure field more symmetric about the whisker (figure 4*a*), resulting in a reduction in VIVs by a factor of 6×.
Miersch *et al*. [42]	
techniques:	Piezoelectric transducer to measure forces during interaction of isolated harbour seal and sea lion whiskers with upstream vortex generator.
findings:	Harbour seal whisker displayed a much higher SNR than sea lion whisker owing to a 10× reduction in VIVs, indicating superior wake detection.
Murphy *et al*. [33]	
techniques:	Laser Doppler vibrometer (LDV) to measure the velocity of the midpoint of harbour seal and sea lion whiskers.
findings:	Similar VIV response for both whiskers, i.e. no effect of undulations.
Bunjevac *et al*. [43]	
techniques:	Snapshot and time-resolved PIV for elephant seal and sea lion whiskers (full length).
findings:	Undulations promoted better mixing within the wake and reduced the turbulence intensity and reversed-flow region compared with the smoother whisker.

the sea lion's chase was more than 4–5 s (compared with approx. 30 s for the harbour seal [14]) and (ii) the trail was curvilinear rather than linear. The blindfolded sea lion also had improved success rates in locating the submarine when the latter was left 'on' when the chase started, suggesting that acoustic cues in conjunction with hydrodynamic cues could be important for this species to follow the trail (compare this with the harbour seal [14], which could trace out the submarine's exact path without requiring any acoustic cues). It is also interesting to note that when a California sea lion was subjected to dipole stimuli underwater (similar to tests conducted on harbour seals [4]), it showed even lower sensing thresholds than the harbour seal at the tested frequencies of 20–30 Hz [52]. The evidence presented above suggests that the California sea lion may well be more sensitive to stimuli at lower speeds or in still water conditions (where VIVs are not expected to be significant) than the harbour seal, but may display a worse performance when executing high-speed long-distance prey tracking. The different lifestyles of *Phocidae* and *Otariidae* could be responsible for the different anatomical features of their whiskers. For instance, *Phocidae* hunt for prey in much deeper waters than *Otariidae* [40], implying that the former would need to forage in lower visibility conditions than the latter, thus necessitating a more sensitive hydrodynamic trail-following system. Indeed, *Phocidae* are known to be far less dependent upon the land than *Otariidae* (e.g. phocid pups must swim when they are a few minutes old while otariid pups remain on land for several months before entering the water) and have a much less developed olfactory modality than *Otariidae* [41]. The differences between the whisker morphology of *Phocidae* and *Otariidae* may thus be linked to the differences in their respective lifestyles and sensory modalities, and the evolution of undulations in the phocid seal whiskers must be seen as an adaptation to their local environments and foraging habits.

Finally, we note that, in addition to the evolutionary significance of wavy whiskers, the relation between the undulating geometry and VIV suppression is of great value in biomimetic technology, as we will discuss later in §5.

3.2. Effect of the angle of attack

The discussion of §3.1 assumed an orientation of the seal whisker wherein its larger dimension (or major axis) was parallel to the direction of water flow. This makes the angle of attack (AOA) equal to zero (e.g. refer to the orientation of the whisker and the ellipse in figure 4*a*), where AOA is defined as the angle between the swimming velocity of the seal and the major axis of the seal whisker. The AOA that the seal uses while following a hydrodynamic trail is, however, not known definitively. It has been assumed so far that the AOA = 0° orientation would be the preferred orientation since this would present the least frontal area to the flow and would hence ensure low drag forces on the whiskers while swimming. However, the AOA value is expected to vary owing to the seal's head movements and water currents [32], and it is important to study how the VIV response of the seal whiskers could change depending upon their orientation. Murphy *et al*. [33] examined the VIV response of individual harbour seal, elephant seal and California sea lion whiskers at three different AOAs equalling 0°, 45° and 90° (the last case represents the situation where the wider dimension of the whisker faces the flow) and found that the whisker vibrations increased in amplitude but decreased in frequency with increasing AOA. Since the vortex-shedding frequency is inversely proportional to the characteristic dimension of the structure (equation 3.1), and since this characteristic dimension (assumed to be the whisker dimension that faces the flow) increases with AOA owing to the elliptical cross-section of the whiskers, the decrease in VIV frequency with increasing AOA seems reasonable. Subsequent PIV measurements conducted in the wake of scaled-up whisker models [44] and real harbour seal whiskers [43] revealed that, at higher AOA, enhanced vortex shedding and higher velocity fluctuations behind the whiskers led to flow instability, which can explain the increase in VIV

amplitude reported by Murphy *et al*. [33]. While an important finding, it is probable that the AOA = 90° orientation is not physically realistic since, in this orientation, the whisker functions as a bluff body and loses the advantages of having an elliptical streamlined shape in the AOA = 0° orientation. Indeed, AOA = 30° was determined as the limit by Wang & Liu [44], within which the benefits of reduced VIVs for an undulating whisker-like structure would be retained.

3.3. Sensing mechanisms

The behavioural experiments reviewed in §2 revealed an exquisite ability of seals to respond to minute flow disturbances and follow hydrodynamic trails long after the escaping object had passed by. The exact mechanisms via which the whisker array performs flow-field measurements to extract information regarding the direction, size, shape and speed of the escaping prey are, however, not well known. It has been suggested [14,42] that seal whiskers vibrate with a characteristic frequency when seals swim, and when the whisker array intercepts a hydrodynamic trail of interest the flow field of the trail changes the vibration frequency of the whiskers. This frequency modulation of the vibrating whiskers, which depends upon the hydrodynamic content encoded within the trail (e.g. direction, speed and type of escaping prey), is then thought to convey the relevant information to the seal via mechanoreceptors in the FSC. The frequency modulation theory is supported by the behavioural experiments conducted by Murphy *et al*. [53], who used an accelerometer to monitor the vibrations of a supraorbital harbour seal whisker (figure 5*a*, left) while the seal tracked a hydrodynamic trail generated artificially. The *in vivo* vibration measurements [53] confirmed a definite broadening of the spectrogram signal when the seal followed a trail compared with when it swam freely (figure 5*a*, right), thus providing empirical evidence for the frequency modulation hypothesis. Finally, we note that the available neurophysiological data [27] obtained from anaesthetized grey and harbour seals indicate that two-thirds of the afferent fibres are rapidly adapting (RA) and responsive to frequencies up to 1000 Hz, indicating the sensory capability of seal whiskers to measure oscillatory hydrodynamic signals over a broadband of frequencies.

Two mechanisms have been proposed in the literature to explain how the seal whisker interacts with vortices in a flow and modulates its vibration frequency, as discussed below.

3.3.1. Slaloming

For a seal whisker to be sensitive to the hydrodynamic trail of an upstream object, it must be able to sense the dominant frequency in the wake of the object. The wake of a swimming fish consists of a chain of staggered 3D vortex structures that resemble a reverse Kármán vortex street (figure 3*d* [23]). In this case, the dominant frequency is the frequency of vortex generation in the reverse Kármán street. Since the wake of a fish contains a predictable flow signature [19] that the seal is capable of interpreting to infer the direction, size and shape of the prey [18,21], it can be postulated that, to extract and interpret relevant information from the wake, the seal whisker's vibrations must be locked in to the dominant frequency of the wake.

Beem & Triantafyllou [39] studied the behaviour of a harbour seal whisker-inspired structure in the wake of a controlled vortex generator using a physical modelling approach. A whisker-like plastic structure was 3D printed according to the dimensions of a real whisker (geometric scaling factor of 20×) and cantilevered to a sensing base that accurately measured the tip displacement of the structure in both the in-flow and cross-flow directions. When the whisker-like structure was placed in open flow without an upstream object, it recorded minimal vibrations (compared with similarly sized circular and elliptical cylinders) owing to VIV suppression, validating previous work conducted with real whiskers [32,42]. However, when the whisker-like structure was placed in the wake of a rigid upstream cylinder (figure 5*b*, top left) that shed vortices approximating those expected in the wake of a real fish, the structure vibrated in the cross-flow direction at much higher amplitudes (up to 30× more) than its open-water response and was successfully 'locked in' to the vortex-shedding frequency of the stimulus. Such 'wake-induced vibrations' (WIVs) persisted even for vortex generator–whisker distances as large as 160× the whisker diameter, with the WIVs always greater than the structure's vibration response in open flow (figure 5*b*, bottom right); in other words, the WIV > VIV condition was always maintained, unlike the circular cylinder (figure 5*b*, top right), where VIV > WIV was observed for many flow speeds and vortex generator–cylinder distances. This implied that the undulating elliptical shape inspired by the harbour seal was always effective in sensing the signal by minimizing its VIV-induced noise.

While the low VIV response of the undulating whisker-inspired structure compared with circular and elliptical cylinders was largely expected (see §3.1), the whisker's ability to be synchronized with the dominant frequency of the wake, even at large separations between the upstream cylinder and the whisker, was intriguing when seen in the context of existing fluid–structure interaction literature. For a comparable case of a flexible downstream circular cylinder excited by a rigid upstream cylinder, the WIVs of the downstream cylinder occur at frequencies equal neither to the dominant frequency of the wake nor to the natural frequency of the cylinder itself [39,55]. The mechanism responsible for the whisker-like structure's lock-in was shown by Beem & Triantafyllou [39] to be due to an elegant 'slaloming' movement undertaken by the whisker-like structure to efficiently extract energy from the upstream vortex generator. During the transverse WIVs, the whisker-like structure first approached the closest oncoming vortex on one side and was pulled towards it owing to the low-pressure region associated with a vortex; then, as the whisker progressed forward, it moved sideways, approaching the next vortex on the other side, again pulled by its low-pressure gradient and so on (figure 5*b*, bottom left). Interestingly, the slaloming mechanism is a commonly adopted strategy by fishes to perform energy-efficient gaiting in the wake of other fishes [2]. Although the experiments were performed on a scaled-up whisker-like model (as opposed to a real harbour seal whisker), the work of Beem & Triantafyllou [39] was significant in that it provided the first mechanistic explanation for the exquisite sensitivity of undulating seal whiskers.

3.3.2. Stick–slip

Muthuramalingam & Bruecker [54] proposed an alternative mechanism of whisker–vortex interaction, analogous to the stick–slip events observed in rat whiskers that have been

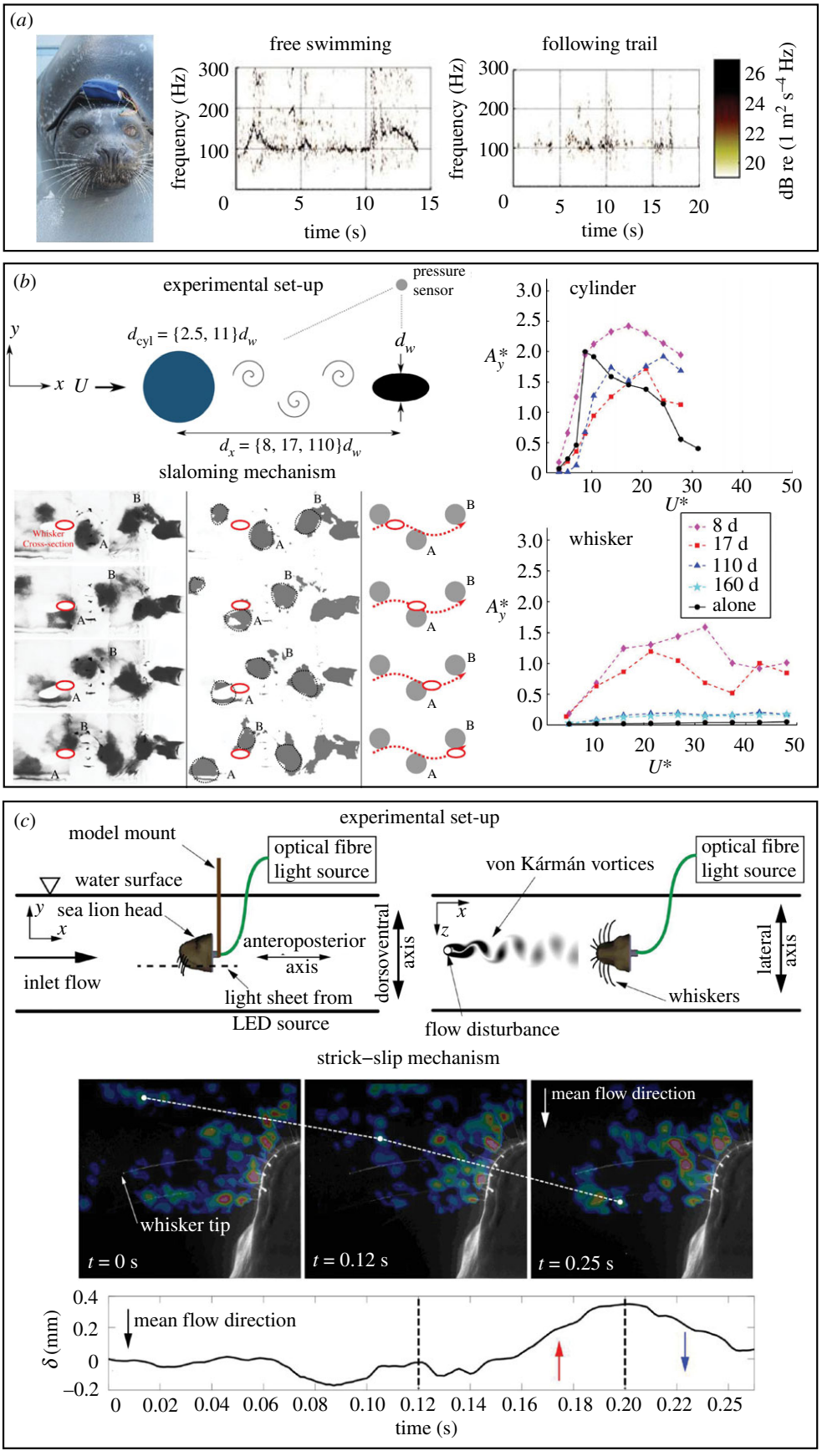

Figure 5. Interaction of seal whiskers with flow vortices. (*a*) *In vivo* vibration measurements conducted on the supraorbital whisker of a harbour seal showing a broadening of the frequency signal when the seal tracked a trail versus when it was freely swimming. Adapted from [53]. (*b*) Slaloming mechanism showing how the whisker can get locked in to the dominant wake frequency, enabling the desired condition of WIV > VIV at all flow speeds (unlike the cylinder). Red ellipse: whisker; A and B: vortices identified using dye visualization; red dotted line: slaloming trajectory of whisker between the wake vortices. The 'alone' curve in the legend (right) indicates the VIV response while the other curves indicate the WIV response at different whisker–stimulus distances. Adapted from [39]. Copyright © 2015 Cambridge University Press. Reprinted with permission. (*c*) Stick–slip mechanism showing the interaction of a whisker with a vortex core (white dot) at three instants. The whisker tip (δ) is seen to 'slip' and move against the flow direction (red arrow) when it contacts the vortex core, following which it 'sticks' again and bends into the flow direction (blue arrow) after the vortex core moves downstream. Adapted from [54].

proposed to help them encode textural information [56]. Using an innovative experimental set-up that comprised a 3D printed sea lion head and optical fibres (illuminated by an external light source) approximating the whiskers on the muzzle, the researchers [54] studied both the in-flow and cross-flow deflection of the whisker-like fibres in steady water flow (i.e. the VIV response) and in the wake of an upstream vortex generator (i.e. the WIV response), as shown in figure 5*c*. The optical fibres mimicking the sea lion whiskers were chosen to have comparable properties and dimensions to those of real whiskers, with the only point of departure being that the fibres were circular in cross-section as opposed to the elliptically shaped sea lion whiskers. This unique experimental set-up also allowed the researchers to observe the interactions of the whisker array with the flow, an approach that improved upon prevalent approaches that only studied isolated whisker behaviour in flow [32,33,42]. Using high-speed camera recordings and PIV measurements, two distinct whisker movements were observed (figure 5*c*, bottom):

(i) Stick: in steady flow, the cantilevered whiskers exhibited a steady bending (along the in-flow direction) caused by drag forces, and vibrated in the cross-flow direction at their natural frequency (approx. 75 Hz) owing to VIVs; and
(ii) Slip: when the whiskers encountered an oncoming vortex ring, they momentarily relaxed their bending owing to the suction effect of the lower pressure associated with the vortex ring; after the vortex ring passed by, they assumed their steady bent profile again, constituting a jerky movement (WIVs) at the same frequency (approx. 2.4 Hz) as that of the approach of oncoming vortices.

A notable difference in this mechanism compared with the slaloming mechanism described in §3.3.1 was that the WIVs triggered by the oncoming vortices in the stick–slip mechanism occurred along the flow direction, as opposed to the cross-flow direction during slaloming.

The differences in the slaloming (figure 5*b*) and stick–slip (figure 5*c*) mechanisms may be attributed to the difference in the stimulus frequencies of the upstream vortex generator used in the two studies [39,54]. Beem & Triantafyllou [39] used wake frequencies of the same order as the natural frequency of their structure, while Muthuramalingam & Bruecker [54] used wake frequencies that were around 35× lower than the whisker-like fibres' natural frequencies. Such a large difference in the wake and natural frequencies is bound to change the WIV dynamics significantly, with the possibility that the whisker may achieve the 'lock-in' state with the wake frequency using different mechanisms depending upon the wake frequency. Further, the whisker shape certainly influences the slaloming ability [39], with circular cross-sections (similar to the ones used by Muthuramalingam & Bruecker [54]) found to be incapable of exhibiting the slaloming movement. Finally, we note some caveats with regards to the physical modelling approach. For instance, it has been observed via video recordings of live seals [32,33] that the whiskers did not discernably bend back as the seals swam at speeds of 0.5–1 m s^{-1}, contrasting the predictions of the physical model [54] where the bending back of the whisker (i.e. the 'stick' phase, an important step in the proposed mechanism) was observed even at lower flow speeds of 0.3 m s^{-1}. It is probable that, in the laboratory experiment of [54], the whisker-like fibres were not attached to the 3D printed sea lion head in the same manner as in the real sea lion, leading to different boundary conditions for the cantilevered whiskers in both cases. It is thus important for a physical model to maintain as much fidelity to the real-life scenario as possible.

We conclude this section by noting that, unlike the fish lateral line [57,58] or the rat whisker [56,59,60] sensory systems, a mechanistic understanding of how the seal senses and interprets the information from hydrodynamic trails is still relatively nascent. The mechanisms [39,54] discussed above represent important steps towards broadening our knowledge, and more such studies (preferably conducted on arrays of real seal whiskers) are warranted to validate existing theories and develop new neurological and fluid mechanical insights.

4. Structure of the seal whisker

The remarkable trail-following ability of seals is enabled in large part by their wavy whisker morphology that suppresses self-induced noise while swimming, as discussed in §3.1. In order to develop predictive biomechanical models that can describe the form–function relationships of the seal whisker system, it is necessary to first measure and quantify the whisker's undulating geometry and material properties that can serve as inputs to such models. The morphometrics of (phocid) seal whiskers is, however, non-trivial owing to the 3D undulations, curvature and taper in the whisker geometry that do not lend themselves to quick measurements using calipers or the optical microscope, but rather necessitate more sophisticated 3D measurement techniques such as computed tomography (CT) scanning. Similarly, the unusual shape of the whiskers with respect to their non-uniform cross-section makes the measurement of mechanical properties (e.g. Young's modulus) a challenge. In this section, we review the geometric models developed to capture the unique morphology of phocid seal whiskers and present available data in the literature on the material properties of whiskers. The effect of the geometry and material properties on the natural frequencies of the whiskers is also discussed.

4.1. Morphometrics

The seal whisker is, in essence, a cantilevered cylinder with a flattened (approximately elliptical) cross-section, displaying a gradual taper from the proximal to the distal end. Fifteen out of eighteen species of seals from the *Phocidae* family [32] display undulations along the whisker length that are manifested as periodic variations in the major and minor axes of the elliptical cross-section, wherein the period (i.e. the wavelength of undulations) is the same for both axes. The major and minor axis undulations appear to be out of phase, i.e. when the major axis reaches its maximum value, the minor axis reaches its minimum value and vice versa, thus maintaining the cross-sectional area roughly consistent between successive undulations [33]. Finally, the whiskers also display significant curvature (roughly in one plane [61]), the direction of which depends upon the species; for instance, in harbour and elephant seals, the curvature is observed in the downstream direction while in sea lions the whisker is curved along the cross-flow direction [33]. Thus, three distinct geometrical aspects can be identified in seal whiskers: undulations, taper and curvature, as illustrated in figure 6*a* for some species [40].

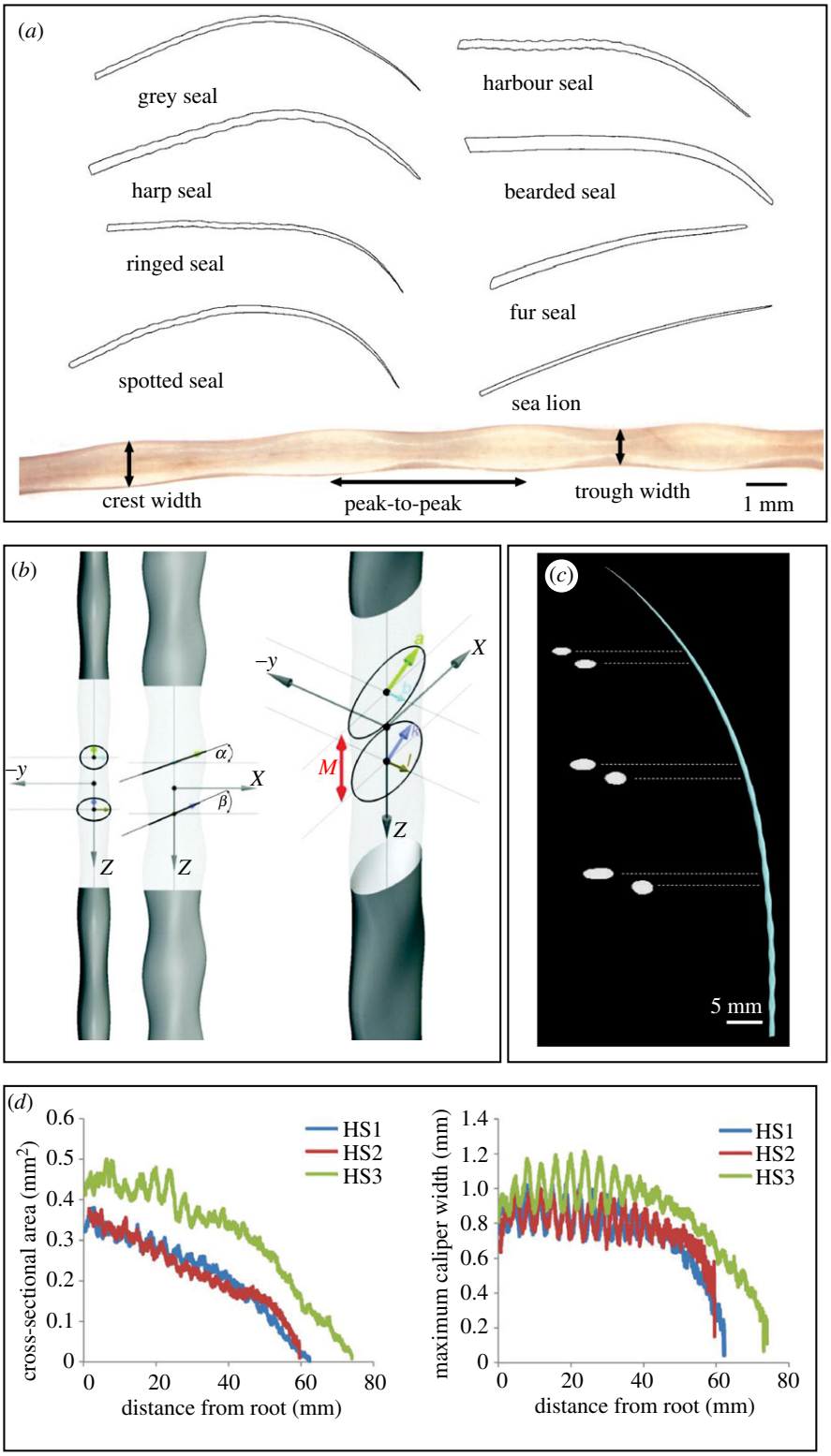

Figure 6. Morphometrics of undulating seal whiskers. (*a*) Two-dimensional outlines of whiskers (both undulating and otherwise) from different seal species, along with basic definitions of undulations. Adapted from [40]. (*b*) Hanke *et al.*'s geometric framework comprising seven parameters that described the whisker undulations. Adapted from [32]. Copyright © 2010 The Company of Biologists. (*c*) Three-dimensional CAD model of an undulating harbour seal whisker obtained using CT scanning. Adapted from [33]. (*d*) Quantification of both undulating and tapering behaviour of three harbour seal (HS) whiskers obtained by CT scanning. Adapted from [33].

Owing to the unique nature of the undulations, morphometrics work has mainly focused on quantifying these undulations and performing comparative studies across different species. Although the undulations are three dimensional in nature and occur along both the major and minor axes, early work focused only on two-dimensional (2D) measurements in the plane containing the wider edge of the whisker owing to ease of laying the whisker flat prior to optical microscopy [40,62]. Specifically, the peak-to-peak distances along both the top and bottom profiles of the whisker (as seen in a 2D view), the crest width and the trough width (figure 6*a*) were measured and reported. Later work used 3D measurement techniques such as CT scanning [33,63] to measure these parameters. Table 3 provides a summary of such measurements conducted in the middle portion of harbour seal whiskers, where the curvature is minimal and the

Table 3. Morphometrics of undulating harbour seal whiskers.

reference	peak-to-peak top (mm)	peak-to-peak bottom (mm)	crest width (mm)	trough width (mm)	crest width/trough width
Hanke *et al*. [32]	1.82[a]	n.a.	1.19	0.95	1.25
Ginter *et al*. [40]	3.27 ± 0.39	3.26 ± 0.40	0.92 ± 0.13	0.73 ± 0.12	1.26
Murphy *et al*. [33]	3.88 ± 0.45	n.a.	1.11 ± 0.88	0.88 ± 0.03	1.27
Rinehart *et al*. [63]	3.44 ± 0.72	3.45 ± 0.73	1.05 ± 0.24	0.83 ± 0.19	1.26

[a]It is likely that this value was mistakenly underreported by a factor of 2 by Hanke *et al*. [32].

taper is negligible, and indicates good consistency in the available morphometrics data for the harbour seal whisker (the most well-studied seal species). An expanded summary containing data for other seal species can be found in electronic supplementary material, table S1, Sheet 2 and is also made publicly available as a GitHub repository (https://github.com/ZhengXingwen/Flow-sensing-mechanisms-and-biomimetic-potential-of-seal-whiskers.git).

Since the data given in table 3 represent 2D measurements that do not fully capture the 3D geometry of the whiskers, a geometric framework [32] comprising seven parameters (a, b, k, l, M, α and β as defined in figure 6*b*) has also been used to report undulation measurements. Here, the undulating whisker is approximated as a 3D surface enveloping two periodically repeating ellipses: the major axis of the first ellipse (semi-major axis = a, semi-minor axis = b) is defined by joining neighbouring crests on the top and bottom profiles of the whisker, while the major axis of the second ellipse (semi-major axis = k, semi-minor axis = l) is defined by joining neighbouring troughs on the top and bottom profiles of the whisker. The two ellipses are inclined with respect to the longitudinal axis of the whisker at angles of α and β, respectively. The alternating repetition of the two ellipses (separated by a distance of M) along the longitudinal axis can be easily converted into a 3D surface model of the whisker using the 'loft' operation commonly used in computer-aided design (CAD) software suites.

The above parameterization of the undulating geometry represents a convenient method of creating a 3D CAD model of the undulating seal whisker via 2D measurements (e.g. using an optical microscope) along both the wide and narrow edges of the flattened whisker. Although originally [32] developed for the harbour seal whisker, this framework was used by Rinehart *et al*. [63] to report elephant seal whisker morphometrics and can also, in principle, be used to report morphometrics of whiskers of other seal species that display undulations. It must be noted, however, that the framework contains many implicit assumptions and hence results in an idealized model of the undulating whisker. For instance, the assumption of two ellipses being inclined at constant angles of α and β does not hold true, with experimental data demonstrating that these angles show a large spread (e.g. from −20° to 20° for harbour seal whiskers [63]) along the length of the whisker. Further, the framework does not account for the taper and curvature of the whisker and is hence only valid for a few undulating wavelengths in the middle section of the whisker. Three-dimensional measurement techniques such as CT scanning [33,63] can generate an exact digital model of the seal whisker (figure 6*c*), from which the properties of interest, e.g. variation of cross-sectional area, major axis dimension, eccentricity (deviation from circularity) and curvature along the whisker length, can be extracted (examples of the first two parameters are shown in figure 6*d* [33]).

A unifying geometric framework, describing the undulations, taper and curvature of whiskers and valid across multiple seal species, is currently lacking and would be beneficial from the point of view of comparative morphometrics and standardization in the reporting of geometric parameters. Recent work [61] has shown that whiskers from across multiple terrestrial and aquatic species (including harbour and grey seals) exhibit curvatures and tapers that can be neatly captured by simple analytical equations. The success of such elegant approaches inspires hope that the undulating geometry of phocid seal whiskers might also be amenable to simple descriptions using general mathematical equations.

4.2. Material properties

The material properties of the keratinous seal whisker, especially its Young's modulus and density, directly influence its frequency characteristics, VIV response and sensitivity to flow. Reliable material property data serve as crucial inputs to numerical models of the whisker's biomechanics during its function as a flow sensor, and are thus essential to develop form–function relations for seal whiskers. In general, very limited data exist on Young's modulus and density measurements of seal whiskers.

Shatz & de Groot [64] used standard microtesting equipment to perform tensile tests on a 60-mm-long harp seal whisker (undulating) and measured Young's modulus to be in the range of 1.8–3.3 GPa. However, no additional information on the testing protocol was provided. Further, approximating the whiskers as tapering rectangular prisms, measuring the whisker length (using a ruler) and width (every 10 mm using a micrometre screw gauge) to estimate the volume, and finally using a microbalance to measure the mass of the whiskers, the authors estimated the whisker density to be 911 ± 100 kg m^{-3}. As far as we are aware, this represents the only data point for the density of seal whiskers in the literature.

Since the seal whiskers are subjected to time-varying loads in their function as underwater flow sensors, Hans *et al*. [65] used the dynamic mechanical analysis (DMA) technique that allowed them to measure the elastic modulus of a harbour seal whisker at different frequencies (1–150 Hz). The DMA technique also allowed for the measurement of the degree of viscoelasticity to help gauge the structural damping of the whisker during VIVs or WIVs. Using DMA to test the properties of four different segments (each 2 cm long) of the whisker, Hans *et al*. [65] reported a gradual reduction in the elastic modulus of the whisker from the proximal end (5–5.5 GPa) to the distal end (1.5–2 GPa), where the

Table 4. Young's modulus measurements of seal whiskers.

source	species	Young's modulus (GPa)	method of measurement
Shatz & de Groot [64]	harp	1.8–3.3	tensile test (Instron 8845 Microtester)
Hans *et al*. [65]	harbour	2–5.5 (distal–proximal)	DMA (0.001% strain at frequencies of 1–150 Hz)
Ginter-Summarell *et al*. [67]	harp	7.62–25.27	point load bending test (MTS Insight 5 SL uniaxial tester,
	harbour	7.53–22.87	25 N load cell)

ranges in parentheses refer to whether the whisker was submerged in saline water prior to testing or whether it was in the dry condition (dry whisker segments displayed a higher modulus). The measurements indicated that the modulus values remained fairly constant up to a frequency of around 93 Hz without any significant viscoelastic effects, implying that standard elastic material models can be used for seal whisker material in numerical simulations. It must, however, be noted that, presumably because of the higher testing frequencies, the strains at which the whiskers were tested (0.001%) were much lower than the bending strains that the whisker is expected to experience during underwater flow sensing. Further, it was surprising that such a drastic change in elastic modulus, from 5 GPa in the proximal segment to 1.5 GPa at the distal segment, was observed, since the keratinous material of the whisker is not expected to show such large variation in properties within a single whisker (compare this result with a similar study done on rat whiskers [66] where the reported Young's modulus values were 2.90 ± 1.25 GPa for the proximal half and 3.96 ± 1.60 GPa for the distal half of the whisker). It is also important to know which cross-sectional dimensions were used to compute the stress reported from the test [65]; if an average cross-sectional area computed over the entire whisker was used, the elastic modulus near the proximal end (where the whisker is wider and thicker than the average) could be overestimated while the elastic modulus near the distal end (where the whisker is narrower and thinner than the average) could be underestimated.

Unlike the uniaxial tests described above [64,65], Ginter-Summarell *et al*. [67] performed bending tests on whiskers obtained from nine different seal species (six with undulations, three without). The measurements entailed applying a point load to the cantilevered whisker (at 25% and 50% of the whisker length measured from the proximal end), obtaining the load–displacement curve from the testing equipment, and finally estimating Young's modulus by fitting it to the predictions of classical beam bending theory. In principle, the bending test represents a more realistic method of determining Young's modulus (compared with uniaxial tests) since the seal whisker undergoes bending (and not uniaxial stretching or compression) during its operation as a flow sensor. Young's modulus obtained from such a test is thus expected to be a better input to biomechanical models of the whisker. However, the methodology [67] described above contained several simplifying assumptions. For instance, the seal whiskers were approximated as circular beams, neglecting the undulations, tapering and, perhaps most importantly, the elliptical cross-section of the whisker, to simplify the calculations using classical beam bending equations. This assumption could be responsible for the large spread observed in the estimated Young's modulus values: for example, depending upon the direction and the point of loading, estimates for Young's modulus were as varied as 11.96, 7.53, 22.87 and 12.07 GPa for the harbour seal whisker [67]. It might be suggested that using finite-element (FE) methods (instead of classical theory) to simulate the whisker bending and using Young's modulus as a 'fudge factor' to fit the FE model predictions to experimental data can result in more accurate and reliable Young's modulus data.

The preceding discussion indicates a general paucity of material property data for seal whiskers. This can be largely attributed to the difficulty of access to seal whiskers for most research groups. Further, the limited material property dataset values do not show good agreement with each other (table 4), suggesting the need for much more research effort into the material characterization of seal whiskers. The material property dataset has been made publicly available as a GitHub repository that will be updated periodically to reflect newer results (https://github.com/ZhengXingwen/Flow-sensing-mechanisms-and-biomimetic-potential-of-seal-whis
kers.git).

4.3. Natural frequency measurements

Seal whiskers function as vibrating cantilevers whose frequency modulations are driven by the information encoded within the hydrodynamic trail that the seal follows, as discussed in §3.3. The geometric and material properties discussed in §§4.1 and 4.2 directly affect the natural (or resonant) frequency of seal whiskers. As an illustration, the natural frequency f_n of a uniform rectangular cantilever (thickness = t, length = L) having a density ρ and Young's modulus of E can be estimated (for bending about the longer axis) to be [68]:

$$f_n = 1.94 \frac{t}{L^2} \sqrt{\frac{E}{\rho}}. \tag{4.1}$$

Although computed for an idealized case of a rectangular cantilever with no undulations, taper or curvature, equation (4.1) is still instructive in demonstrating the dependence of the whisker geometry (length and thickness) and properties (Young's modulus and density) on its natural frequency. For instance, the inverse dependence of natural frequency on the square of cantilever length indicates that the whiskers on the seal muzzle must have very different natural frequencies owing to the large differences in whisker lengths (e.g. 33–105 mm for harp seals [64]). Shatz & de Groot [64] argued that the differently sized whiskers on the seal's muzzle could be sensitive to different frequency bands of hydrodynamic stimuli, taking inspiration from similar ideas in the rat whisker literature [60,69]. The researchers [64] experimentally

measured the resonant frequencies of harp seal whiskers of different lengths (33–105 mm) by exciting them in the air using a variable-frequency acoustic source. A corresponding FE model that calculated the eigenfrequencies of the respective seal whiskers was developed by approximating the seal whisker as a tapering rectangular cantilever (using $E = 2.9$ GPa and $\rho = 911$ kg m^{-3}), with very good agreement with the experimentally measured frequencies. An interesting consequence of the frequency selectivity hypothesis is that individual whiskers can amplify hydrodynamic signals near their respective natural frequencies by achieving resonance, thus allowing the seal to sense and encode a broad band of hydrodynamic stimuli. This transduction mechanism is analogous to the 'differential resonance' theory proposed to explain how rats use their whisker arrays to encode tactile stimuli [60,69].

The natural frequencies measured by Shatz & de Groot [64] were in the range of 20–200 Hz and showed good agreement with available data in the literature, e.g. the *in vivo* measurements conducted on the supraorbital whisker of a harbour seal during behavioural experiments (100–300 Hz [53]) and the measurements conducted on isolated harbour seal whiskers in the air using a mini-shaker apparatus (30–175 Hz [65]). Although inter-study [53,64,65] comparisons are not ideal owing to differences in the seal species and whisker sizes, all the reported ranges indicate that the whiskers are ideally attuned to sense frequencies typically encountered in hydrodynamic trails (at least 100 Hz [17]). Finally, it is important to note that the boundary condition at the whisker base can have a strong effect on the resulting natural frequency. Measurements conducted on isolated whiskers [64,65] usually involve a rigid clamping of the whisker's base that differs significantly from the real-world scenario, wherein the seal whisker is embedded (up to 10–15 mm [31]) in the soft tissue constituting the follicle. Such differences in the boundary condition can change the natural frequencies by up to a factor of 2 [64] and must be accounted for in biomechanical models of the seal whisker.

Finally, we note that limited data exist on the internal structure of the seal whisker. Hans *et al*. [65] observed a hollow elliptical region when they transversely sectioned a harbour seal whisker near its centre. The presence of a centrally connected cavity in seal whiskers, if it exists, is expected to affect the dynamic properties (e.g. natural frequency) of the whiskers. Since a low-density medullar region (often approximated as a hollow conical region) that can be up to 30% of the base diameter and can extend up to 80% of the whisker length [70] is known to exist in rat whiskers, it appears worthwhile to investigate whether a similar region could also exist in the seal whisker.

5. Biomimetics

The extraordinary trail-following ability of seals enabled by their low-noise flow-sensing whiskers has exciting consequences for biomimetic engineering applications. For instance, the underwater prey detection ranges of seals (estimated to be approx. 180 m [14]) and echolocating dolphins (107–173 m [20]) are similar, implying that the passive sensing strategy employed by seals can inspire much cheaper and energy-saving alternatives to currently used sound navigation and ranging (SONAR) systems. Similarly, the VIV suppression capability of the undulating geometry of seal whiskers can be used to design vibration-resistant structures in high *Re* flow environments. In this section, we present an overview of some recent technological developments that took inspiration from seal whiskers.

5.1. Whisker-inspired flow sensors

Inspired by the VIV suppression ability of the seal whisker, a variety of flow sensors featuring whisker-like structures have been designed and fabricated in recent years. The biomimetic flow sensor design generally consists of a high-aspect-ratio structure (inspired by the whisker) mounted on a sensing base (inspired by the innervated whisker follicle). When the whisker-inspired structure encounters a flow stimulus, steady and/or dynamic, it deflects and produces a high bending stress in the sensing base that is transduced into a measurable electric signal that is proportional to the flow stimulus. The sensing principle that converts the mechanical deformation at the sensing base into a voltage output can be resistive (e.g. using strain gauges [71]), piezoresistive (e.g. using graphene as the sensing material [72]), capacitive [73,74], piezoelectric [75,76] or optoelectronic [77] in nature. The rationale behind the bioinspired design is that the whisker-like undulating shape reduces noise that would usually occur as a result of VIVs (e.g. in the case of a circular cylinder without undulations), thus enhancing the SNR of the flow sensors in high *Re* flows.

To measure the flow velocity and recognize the flow direction, Beem *et al*. [71] developed a flow sensor using a scaled-up (30×) whisker-like undulating structure. The 3D printed polymer whisker was mounted on a rubber diaphragm attached to four bend sensors. The vibrations of the whisker induced deformation in the four bend sensors, generating voltage signals that were precisely calibrated to the vibration amplitude and frequency of the whisker. Further, the four-sensor design allowed the vibration direction of the whisker (i.e. in-flow or cross-flow) to be determined easily. The whisker-inspired sensor was mounted on a testbed and used for measuring the flow velocity and in the sea (figure 7*a*), and its performance was found to match well with the measurements of a commercial flow sensor mounted on the testbed [71]. The whisker-inspired sensor was also capable of detecting vortex wakes generated under laboratory conditions (similar to the work by the same authors [39] discussed earlier in §3.3.1) and thus showed promise for autonomous underwater vehicle (AUV) navigation using passive sensing.

By contrast to Beem *et al*.'s work [71], where scaled-up versions of whisker sensors were developed, Kottapalli *et al*. [75,76] developed a miniaturized whisker-inspired sensor, as shown in figure 7*b*. The whisker-inspired structure (3D printed using stereolithography at the true scale) was mounted onto a piezoelectric $Pb(Zr_{0.52}Ti_{0.48})O_3$ membrane fabricated using microelectromechanical systems (MEMS) technology (figure 7*b*, left). Compared with its cylindrical counterpart (namely, a sensor featuring a cylinder of similar dimensions with no undulations), the whisker-inspired sensor displayed a VIV response up to 50× lower than the circular cylinder in steady flow [76]. The sensor was also experimentally characterized using a vibrating sphere (35 Hz) stimulus generating a dipole flow, where it displayed impressive flow-sensing thresholds as low as 193 µm s^{-1} (figure 7*b*, right), on a par with the flow-sensing performance of real harbour seals [4]. The use of a

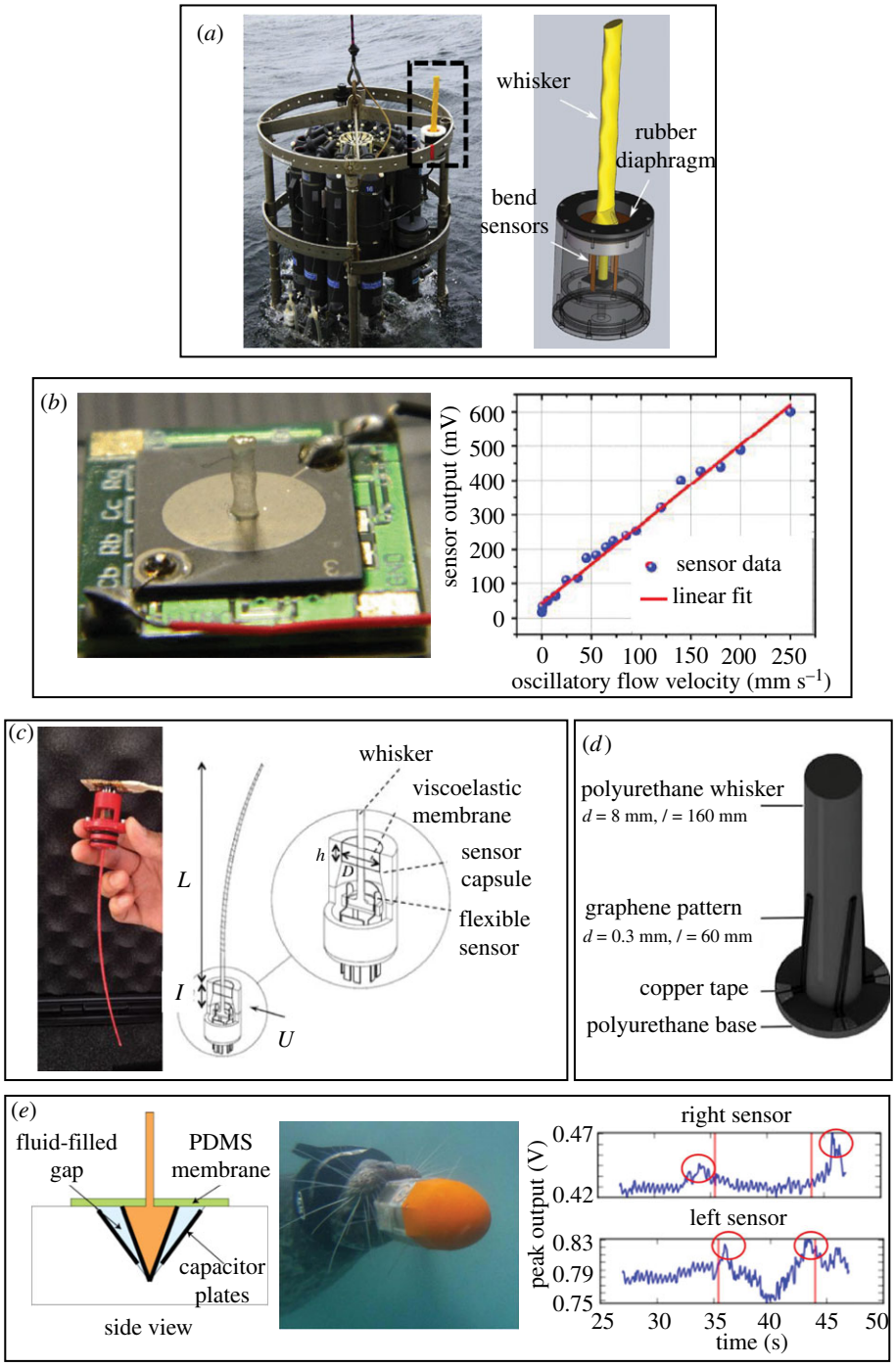

Figure 7. Biomimetic flow sensors. (*a*) Scaled-up whisker-like directional flow sensor deployed in the ocean. Adapted from [71]. Copyright © 2013 IOP Publishing. Reprinted with permission. (*b*) 3D printed whisker-inspired structure (to scale) mounted on a MEMS piezoelectric sensing base to realize a self-powered flow sensor with linear response and very low sensing thresholds of 193 µm s^{-1}. Adapted from [75,76]. Copyright © 2014–15, IEEE. Reprinted with permission. (*c*) Whisker-inspired flow sensor with a soft sensing base modelled after the whisker FSC. Left image adapted from [78]. Copyright © 2017 Springer Nature. Reprinted with permission. Right image adapted from [79]. Copyright © 2013 IEEE. Reprinted with permission. (*d*) Flexible whisker-inspired flow sensor with four graphene strain gauge patterns at the base fabricated using a one-step multi-material 3D printing process. Adapted from [72]. Copyright © 2018 Mary Ann Liebert, Inc. (*e*) Capacitive whisker-like flow-sensing array mounted on a live seal that recorded signals while following hydrodynamic trails. The left and right sensors recorded a signal (circled in red) upon interaction with the vortices in the wake street. Left image adapted from [74]. Copyright © 2011 IEEE. Reprinted with permission. Middle and right images adapted from [80]. Copyright © 2011 IOP Publishing. Reprinted with permission.

MEMS-fabricated piezoelectric sensing membrane [75,76] made the sensors small, self-powered and highly sensitive to dynamic excitation over a broad frequency range (up to 23.3 kHz).

In addition to the whisker undulations that were the focus of the biomimetic sensors described above, Alvarado *et al.* [79,81,82] also focused on the FSC that houses the innervated whisker base (figure 7*c*). This represented a novel investigation because the soft follicle had hitherto been largely neglected in whisker-inspired flow sensor designs. Using silicone rubber to mimic the soft tissue and musculature in the FSC, commercially obtained flexible bend sensors to measure whisker displacement and fused deposition modelling (FDM) to 3D print a complete harbour seal whisker-inspired structure (including undulations, tapering and curvature) to scale, Alvarado *et al.* [79,81] realized a whisker-inspired flow sensor that displayed less noise than comparable cylinder-shaped

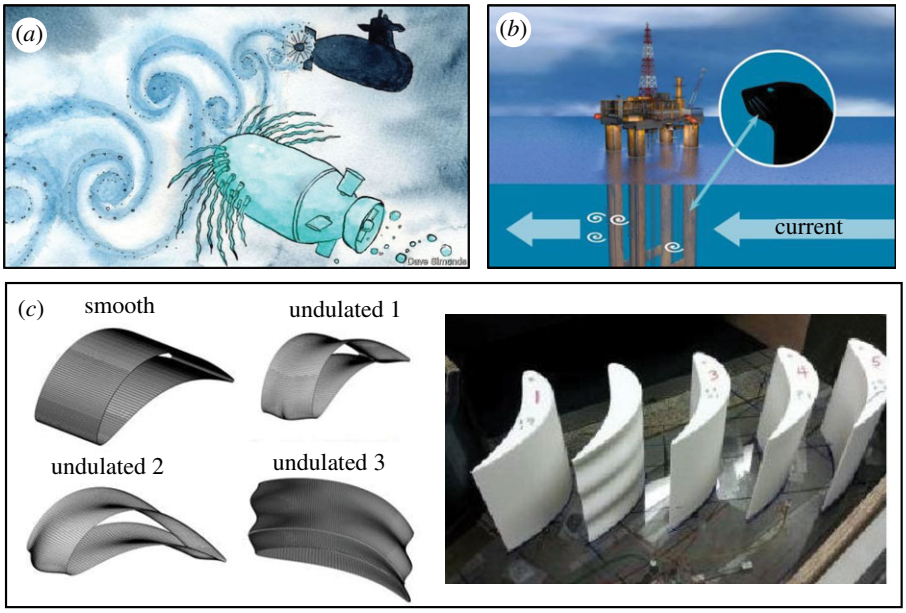

Figure 8. Whisker-inspired engineering applications. (*a*) Artistic vision of a futuristic seal-inspired AUV (credit: Dave Simonds). From [87]. Reprinted with permission. (*b*) Undulating whisker-like offshore structures to reduce vibrations and fatigue-induced failure (credit: Jack Cook and Eric S. Taylor, WHOI Graphics Services). From [88]. Copyright © 2016 Woods Hole Oceanographic Institution. Reprinted with permission. (*c*) Undulating turbine blades developed at the NASA Glenn Research Center resulting in fuel savings of 5%. Adapted from [89]. Copyright © 2015 ASME. Reprinted with permission.

sensors while performing underwater flow measurements [81]. More importantly, by developing a lumped-parameter model for the bioinspired FSC [79,81], the authors were able to tune the sensor characteristics (such as sensitivity and resonant frequency) by varying the material and geometric properties of both the flexible sensing base and the rigid whisker-like structure. The work was significant from the point of view of establishing the important relations between the cantilevered whisker's soft sensing base and its flow-sensing performance, especially since seals are known to protract their whiskers (presumably by stiffening the FSC muscles) when following a hydrodynamic trail [4,18]. A good summary of the whisker and FSC-inspired sensor design and model can be found in [78].

Gul *et al*. [72] developed a fully 3D printed whisker-inspired polymer sensor with four graphene patterns perpendicular to each other (figure 7*d*). The displacement of the whisker-inspired structure in any direction changed the electrical resistance of the graphene patterns at the whisker base, and this phenomenon was used to demonstrate the sensor's capability of detecting both clockwise and anti-clockwise vortices generated by an artificial flapping fin. The work of Gul *et al*. [72] demonstrated the potential of leveraging recent developments in 3D printing (e.g. multi-material deposition) to fabricate low-cost bioinspired sensors in a single step. Further, the use of high-gauge factor [83] graphene as the sensing material and flexible polyurethane as the structural material resulted in high sensitivities, with the whisker recording an impressive 1180% resistance change while detecting underwater vortices (comparable graphene-based flexible flow sensors typically display resistance changes of around approx. 50% [84,85] in normal operation). Although the whisker-inspired structure itself was a simple cylinder, the methodology [72] is general enough to be extended for fabricating an undulating whisker-shaped sensor.

The sensors described above were typically tested in laboratory conditions (with the exception of Beem *et al*. [71]). Eberhardt *et al*. [80] used a unique testing protocol whereby they trained a harbour seal to carry their (non-undulating) whisker-inspired flow-sensing system using its teeth while tracking a moving stimulus (vibrating sphere or a robotic submarine) inside a water tank. The wireless sensing system, termed 'wake information detection and tracking system' (WIDTS), comprised a radial array of eight whisker-inspired capacitive sensors (figure 7*e*, left) developed in their prior work [73,74]. Eberhardt *et al*. [80] were thus able to test the WIDTS against the wake encountered by a real seal (figure 7*e*, middle) during trail-following tasks. Using concurrent and synchronized data from an overhead camera and the WIDTS, the researchers observed that the WIDTS registered a signal (in the form of a voltage spike) whenever the seal intersected the hydrodynamic wake of the object in front of it (figure 7*e*, right), and were able to identify the direction of intersection (i.e. whether the seal made contact with the trail using the left or right side of its muzzle) owing to the use of multiple radially arranged whisker-like sensors.

The work of Eberhardt *et al*. [80] represents the first attempt at realizing robotic whiskers inspired by the seal but also highlights the practical challenges (e.g. unwanted noise due to irrelevant hydrodynamic events, incomplete recovery to the sensor baseline output, water leaks and corrosion) involved in implementing an underwater sensing system. Although erstwhile studies mainly focused on the design and fabrication of whisker-inspired sensors, the work of Eberhardt *et al*. [80] also underscores the crucial role of signal-processing algorithms in encoding the seemingly noisy sensor output. Recent work [86] has demonstrated the utility of bioinspired flow sensors in solving source-seeking tasks for autonomous robots on land using airflow gradient measurements, and similar approaches using reliable whisker-inspired sensors and robust algorithms (source-seeking, trail following, object localization, obstacle avoidance, navigation and so on) will prove to be useful in realizing seal-inspired AUVs (figure 8*a*).

5.2. Engineering applications

The ability of the undulating whisker shape to suppress VIV-induced lift and drag forces can inspire applications in industries where fluid–structure interactions at high *Re* are

common. For instance, offshore structures such as underwater cables and oil platform bases could be designed in the form of a whisker-like wavy cylinder to reduce vibrations and the risk of failure due to structural fatigue, as shown in figure 8*b* [88]. A more concrete application was demonstrated by researchers at the NASA Glenn Research Center [89]. Inspired by the literature on drag and VIV suppression exhibited by the harbour seal whisker, the researchers took inspiration from the 3D geometric parameters of harbour seal whiskers to create undulating power turbine blades (figure 8*c*). CFD simulations and wind tunnel tests ($Re \sim 100\,000$) confirmed that the seal whisker-inspired turbine blade led to a drag reduction of up to 50% with expected fuel savings of around 5%. The results [89] conclusively proved the biomimetic potential of using whisker-inspired undulating shapes in engineering applications.

It is worth asking whether the undulating shapes exhibited by whiskers of phocid seals are optimally suited to suppress VIVs. For instance, what particular benefits does a harbour seal whisker-inspired shape offer in comparison with a wavy [37] or 'bumpy [38]' cylinder in reducing drag and lift forces? Recent work by Liu *et al*. [49] and Lyons *et al*. [50] addressed this question by systematically studying the effects of the geometric parameters of undulating seal whiskers on their drag and lift coefficients using CFD simulations. The aim of these studies was to understand which geometric parameters had the strongest effect on the seal's VIV suppression capabilities. Such numerical optimization studies, in conjunction with experiments conducted with 3D printed seal whiskers of the corresponding geometries, will help enable better VIV-suppressing designs for biomimetic structures.

6. Summary and future directions

Behavioural experiments conducted on real seals for over two decades have demonstrated remarkable hydrodynamic feats such as the capability of following the hydrodynamic trail of an object, without any visual or auditory cues, several seconds after the object has passed by. Such extraordinary behaviour is enabled by seal whiskers that function as ultrasensitive flow sensors. The array of whiskers on the seal muzzle allows the seal to be sensitive to the tiniest of flow disturbances (approx. 245 µm s^{-1}) in the wake of escaping prey, and this flow sensory modality can complement (or even substitute for) the sense of vision in low-visibility conditions. An extensive body of experiments and numerical simulations conducted on isolated seal whiskers has established that the unique undulating shape of seal whiskers reduces VIVs and allows the whiskers to be still when the seal swims, thus enhancing the whiskers' SNR while functioning as flow sensors. The whiskers sense the lingering vortices in the wake of an escaping prey by 'locking in' to the frequencies within the reverse Kármán vortex street that is typical of fish wakes. Two mechanisms, slaloming and stick–slip, have been proposed to explain how the whisker interacts with wake vortices to achieve frequency modulation based on the dominant wake frequency. However, a broad understanding of how the seal conducts multi-point velocity measurements within a hydrodynamic trail using its array of whiskers, and then interprets and processes this information to deduce the size, shape and direction of the escaping prey, is still lacking and not yet at the level of maturity seen in the fish lateral line and rat whisker literature. A major reason for this could be the relative difficulties of performing behavioural and neurophysiological experiments on real seals, compared with fishes and rats.

In order to study the form–function relationships of undulating seal whiskers, the geometric and material properties of seal whiskers have been characterized for several seal species. The geometric framework proposed by Hanke *et al*. [32] (consisting of seven geometric parameters) has been a popular choice in the literature to report whisker undulations and to develop idealized 3D models of the whisker. Material properties data, however, were seen to be limited, presumably because of difficulties of access to real seal whiskers. Finally, the biomimetic potential of the undulating seal whiskers in the design of low-noise flow sensors and vibration-resistant offshore structures is beginning to be fulfilled.

Following a comprehensive and critical review of the multidisciplinary literature on seal whiskers, we identify the following directions as promising for future research in this field.

(i) Although behavioural experiments with live seals have been performed, the *in situ* behaviour of the whiskers when the seal follows a trail is still uncertain. For instance, it is not known with certainty what AOA the seal uses when following its prey. Further, the vibration behaviour of multiple whiskers within an artificially generated wake can help validate current theories of whisker–vortex interactions. The *in vivo* experiments of Murphy *et al*. [53], wherein the vibrations of a supraorbital whisker were monitored using an accelerometer tag while the harbour seal followed an object, represent a promising paradigm for future work, since such experiments ensure a non-invasive method of vibration measurements. Recent technological advances in ultralightweight strain sensors, e.g. electrospun nanofibres [90,91], can allow the vibrations of multiple whiskers to be measured *in situ* without interfering with the whisker's dynamics and ensuring minimal distress to the animal.

(ii) So far, laboratory tests have predominantly focused on the interaction of isolated excised whiskers (or whisker-like structures) with steady water flow. However, the interactions of a single whisker with water flow could be different from the real-life scenario, where the array of whiskers (protracted forward) on the muzzle interact with the flow. The effect of the interaction of an array of whiskers with the water flow on the resulting VIV and WIV response of the whiskers is an interesting problem that has not been addressed yet in the literature.

(iii) Since the undulating whisker shape represents a truly unique geometry not observed in any whiskered mammals apart from *Phocidae*, much research effort has understandably been directed towards understanding the benefits conferred by this geometric feature on flow-sensing. This has occurred, however, at the expense of other geometric features, namely curvature and taper, that are also expected to affect the whisker's operation. The importance of the flexibility gradient offered by a tapering whisker for tactile sensing and 3D mapping is well known in the rat whisker literature [92–94], and it is conceivable that the taper in the seal whiskers can offer similar operational

advantages, e.g. to ease slaloming through a train of vortices, for seal whiskers.

(iv) A more comprehensive database of the material properties of seal whiskers, especially Young's modulus and density, is needed to inform reliable biomechanical models of the whisker. The current data are scarce and show large variation. Further, the internal structure of the whisker, especially with respect to the presence (or absence) of a centrally connected hollow region akin to the rat whisker, merits further investigation for a more complete picture of whisker dynamics.

(v) Finally, the idea of 'robotic seals' equipped with artificial whisker-like sensors that autonomously follow hydrodynamic trails in low-visibility conditions (figure 8*a*) will represent a significant advancement in the field of biomimetic robotics and underwater navigation. The vision is undoubtedly ambitious and will require interdisciplinary efforts across the fields of sensory biology, fluid dynamics, control theory, robotics and sensor design and fabrication. The successful development of robotic fishes realized using an array of lateral line-inspired sensors [95–97] inspires hope that the vision of seal-inspired underwater robots can become a reality in the coming years.

Data accessibility. The datasets supporting this article have been uploaded as part of the electronic supplementary material and are also made available publicly as a GitHub repository (https://github.com/ZhengXingwen/Flow-sensing-mechanisms-and-biomimetic-potential-of-seal-whiskers.git).

Authors' contributions. X.Z. and A.M.K. performed the literature review and wrote the manuscript. M.C. and A.G.P.K. edited the manuscript and supervised the project. All authors gave final approval for publication and agree to be held accountable for the work performed herein.

Competing interests. We declare we have no competing interests

Funding. A.G.P.K. gratefully acknowledges funding from the University of Groningen's start-up grant. A.M.K. was supported by the ITEA DayTime project (grant agreement no. ITEA-2018-17030-Daytime). M.C. gratefully acknowledges funding from the European Research Council (grant no. ERC-CoG-771687) and the Netherlands Organization for Scientific Research (grant no. NWO-vidi-14134).

Acknowledgements. The authors gratefully acknowledge helpful discussions with the veterinarians at the Zeehondencentrum (Pieterburen, The Netherlands) and thank the referees for their constructive comments that significantly enhanced the quality of this review paper.

References

1. Bleckmann H, Klein A, Meyer G. 2012 Nature as a model for technical sensors. In *Frontiers in sensing: from biology to engineering* (eds FG Barth, JAC Humphrey, MV Srinivasan), pp. 3–18. Vienna, Austria: Springer Vienna.
2. Triantafyllou MS, Weymouth GD, Miao J. 2016 Biomimetic survival hydrodynamics and flow sensing. *Annu. Rev. Fluid Mech.* **48**, 1–24. (doi:10.1146/annurev-fluid-122414-034329)
3. Kroese ABA, der Zalm JM, den Bercken J. 1978 Frequency response of the lateral-line organ of *Xenopus laevis*. *Pflüg. Arch.* **375**, 167–175. (doi:10.1007/BF00584240)
4. Dehnhardt G, Mauck B, Bleckmann H. 1998 Seal whiskers detect water movements. *Nature* **394**, 235–236. (doi:10.1038/28303)
5. Soares D. 2002 An ancient sensory organ in crocodilians. *Nature* **417**, 241–242. (doi:10.1038/417241a)
6. Kottapalli AGP, Asadnia M, Miao J, Triantafyllou MS. 2017 *Biomimetic microsensors inspired by marine life*. Basle, Switzerland: Springer International Publishing.
7. Berta A. 2018 Pinnipeds. In *Encyclopedia of marine mammals* (eds B Würsig, JGM Thewissen, K Kovacs), pp. 733–740. Cambridge, MA: Academic Press.
8. Williams TM, Kooyman GL. 1985 Swimming performance and hydrodynamic characteristics of harbor seals *Phoca vitulina*. *Physiol. Zool.* **58**, 576–589. (doi:10.1086/physzool.58.5.30158584)
9. Dehnhardt G, Kaminski A. 1995 Sensitivity of the mystacial vibrissae of harbour seals (*Phoca vitulina*) for size differences of actively touched objects. *J. Exp. Biol.* **198**, 2317–2323. (doi:10.1242/jeb.198.11.2317)
10. Hyvärinen H. 1989 Diving in darkness: whiskers as sense organs of the ringed seal (*Phoca hispida saimensis*). *J. Zool.* **218**, 663–678. (doi:10.1111/j.1469-7998.1989.tb05008.x)
11. Newby TC, Hart FM, Arnold RA. 1970 Weight and blindness of harbor seals. *J. Mammal.* **51**, 152. (doi:10.2307/1378544)
12. Renouf D. 1979 Preliminary measurements of the sensitivity of the vibrissae of harbour seals (*Phoca vitulina*) to low frequency vibrations. *J. Zool.* **188**, 443–450. (doi:10.1111/j.1469-7998.1979.tb03428.x)
13. Renouf D. 1979 Fishing in captive harbour seals (*Phoca vitulina concolor*): a possible role for vibrissae. *Neth. J. Zool.* **30**, 504–509. (doi:10.1163/002829680X00122)
14. Dehnhardt G, Mauck B, Hanke W, Bleckmann H. 2001 Hydrodynamic trail-following in harbor seals (*Phoca vitulina*). *Science* **293**, 102–104. (doi:10.1126/science.1060514)
15. Schulte-Pelkum N, Wieskotten S, Hanke W, Dehnhardt G, Mauck B. 2007 Tracking of biogenic hydrodynamic trails in harbour seals (*Phoca vitulina*). *J. Exp. Biol.* **210**, 781–787. (doi:10.1242/jeb.02708)
16. Mills FHJ, Renouf D. 1986 Determination of the vibration sensitivity of harbour seal *Phoca vitulina* (L.) vibrissae. *J. Exp. Mar. Bio. Ecol.* **100**, 3–9. (doi:10.1016/0022-0981(86)90151-6)
17. Bleckmann H, Breithaupt T, Blickhan R, Tautz J. 1991 The time course and frequency content of hydrodynamic events caused by moving fish, frogs, and crustaceans. *J. Comp. Physiol. A* **168**, 749–757. (doi:10.1007/BF00224363)
18. Wieskotten S, Dehnhardt G, Mauck B, Miersch L, Hanke W. 2010 Hydrodynamic determination of the moving direction of an artificial fin by a harbour seal (*Phoca vitulina*). *J. Exp. Biol.* **213**, 2194–2200. (doi:10.1242/jeb.041699)
19. Spedding GR. 2014 Wake signature detection. *Annu. Rev. Fluid Mech.* **46**, 273–302. (doi:10.1146/annurev-fluid-011212-140747)
20. Au WWL, Benoit-Bird KJ, Kastelein RA. 2007 Modeling the detection range of fish by echolocating bottlenose dolphins and harbor porpoises. *J. Acoust. Soc. Am.* **121**, 3954. (doi:10.1121/1.2734487)
21. Wieskotten S, Mauck B, Miersch L, Dehnhardt G, Hanke W. 2011 Hydrodynamic discrimination of wakes caused by objects of different size or shape in a harbour seal (*Phoca vitulina*). *J. Exp. Biol.* **214**, 1922–1930. (doi:10.1242/jeb.053926)
22. Krüger Y, Hanke W, Miersch L, Dehnhardt G. 2018 Detection and direction discrimination of single vortex rings by harbour seals (*Phoca vitulina*). *J. Exp. Biol.* **221**, jeb170753. (doi:10.1242/jeb.170753)
23. Drucker EG, Lauder GV. 2002 Experimental hydrodynamics of fish locomotion: functional insights from wake visualization. *Integr. Comp. Biol.* **42**, 243–257. (doi:10.1093/icb/42.2.243)
24. Niesterok B, Krüger Y, Wieskotten S, Dehnhardt G, Hanke W. 2017 Hydrodynamic detection and localization of artificial flatfish breathing currents by harbour seals (*Phoca vitulina*). *J. Exp. Biol.* **220**, 174–185. (doi:10.1242/jeb.148676)
25. Murphy CT, Reichmuth C, Mann D. 2015 Vibrissal sensitivity in a harbor seal (*Phoca vitulina*). *J. Exp. Biol.* **218**, 2463–2471. (doi:10.1242/jeb.118240)
26. Engelmann J, Hanke W, Mogdans J, Bleckmann H. 2000 Hydrodynamic stimuli and the fish lateral line. *Nature* **408**, 51–52. (doi:10.1038/35040706)
27. Dykes RW. 1975 Afferent fibers from mystacial vibrissae of cats and seals. *J. Neurophysiol.* **38**, 650–662. (doi:10.1152/jn.1975.38.3.650)

28. Bowen WD, Tully D, Boness DJ, Bulheier BM, Marshall GJ. 2002 Prey-dependent foraging tactics and prey profitability in a marine mammal. *Mar. Ecol. Prog. Ser.* **244**, 235–245. (doi:10.3354/meps244235)
29. Marshall CD, Amin H, Kovacs KM, Lydersen C. 2006 Microstructure and innervation of the mystacial vibrissal follicle-sinus complex in bearded seals, *Erignathus barbatus* (Pinnipedia: Phocidae). *Anat. Rec. Part A Discov. Mol. Cell. Evol. Biol.* **288A**, 13–25. (doi:10.1002/ar.a.20273)
30. McGovern KA, Marshall CD, Davis RW. 2015 Are vibrissae viable sensory structures for prey capture in northern elephant seals, *Mirounga angustirostris*? *Anat. Rec.* **298**, 750–760. (doi:10.1002/ar.23061)
31. Jones A, Marshall CD. 2019 Does vibrissal innervation patterns and investment predict hydrodynamic trail following behavior of harbor seals (*Phoca vitulina*)? *Anat. Rec.* **302**, 1837–1845. (doi:10.1002/ar.24134)
32. Hanke W, Witte M, Miersch L, Brede M, Oeffnet J, Michael M, Hanke F, Leder A, Dehnhardt G. 2010 Harbor seal vibrissa morphology suppresses vortex-induced vibrations. *J. Exp. Biol.* **213**, 2665–2672. (doi:10.1242/jeb.043216)
33. Murphy CT, Eberhardt WC, Calhoun BH, Mann KA, Mann DA. 2013 Effect of angle on flow-induced vibrations of pinniped vibrissae. *PLoS ONE* **8**, e69872. (doi:10.1371/journal.pone.0069872)
34. White FM. 2011 *Fluid mechanics*, 7th edn. New York, NY: McGraw-Hill.
35. Choi H, Jeon WP, Kim J. 2008 Control of flow over a bluff body. *Annu. Rev. Fluid Mech.* **40**, 113–139. (doi:10.1146/annurev.fluid.39.050905.110149)
36. Zdravkovich MM. 1981 Review and classification of various aerodynamic and hydrodynamic means for suppressing vortex shedding. *J. Wind Eng. Ind. Aerodyn.* **7**, 145–189. (doi:10.1016/0167-6105(81)90036-2)
37. Lam K, Wang FH, Li JY, So RMC. 2004 Experimental investigation of the mean and fluctuating forces of wavy (varicose) cylinders in a cross-flow. *J. Fluids Struct.* **19**, 321–334. (doi:10.1016/j.jfluidstructs.2003.12.010)
38. Owen J, Bearman P, Szewczyk A. 2001 Passive control of VIV with drag reduction. *J. Fluids Struct.* **15**, 597–605. (doi:10.1006/jfls.2000.0358)
39. Beem HR, Triantafyllou MS. 2015 Wake-induced 'slaloming' response explains exquisite sensitivity of seal whisker-like sensors. *J. Fluid Mech.* **783**, 306–322. (doi:10.1017/jfm.2015.513)
40. Ginter CC, DeWitt TJ, Fish FE, Marshall CD. 2012 Fused traditional and geometric morphometrics demonstrate pinniped whisker diversity. *PLoS ONE* **7**, e34481. (doi:10.1371/journal.pone.0034481)
41. Renouf D. 1991 Sensory reception and processing in Phocidae and Otariidae. In *The behaviour of pinnipeds* (ed. D Renouf), pp. 345–394. Dordrecht, The Netherlands: Springer Netherlands.
42. Miersch L, Hanke W, Wieskotten S, Hanke FD, Oeffner J, Leder A, Brede M, Witte M, Dehnhardt G. 2011 Flow sensing by pinniped whiskers. *Phil. Trans. R. Soc. B* **366**, 3077–3084. (doi:10.1098/rstb.2011.0155)
43. Bunjevac J, Turk J, Rinehart A, Zhang W. 2018 Wake induced by an undulating elephant seal whisker. *J. Vis.* **21**, 597–612. (doi:10.1007/s12650-018-0484-4)
44. Wang S, Liu Y. 2016 Wake dynamics behind a seal-vibrissa-shaped cylinder: a comparative study by time-resolved particle velocimetry measurements. *Exp. Fluids* **57**, 1–20. (doi:10.1007/s00348-016-2117-9)
45. Wang S, Liu YZ. 2017 Flow structures behind a vibrissa-shaped cylinder at different angles of attack: complication on vortex-induced vibration. *Int. J. Heat Fluid Flow* **68**, 31–52. (doi:10.1016/j.ijheatfluidflow.2017.09.006)
46. Chen WL, Min XW, Gao DL, Guo AX, Li H. 2018 Experimental investigation of aerodynamic forces and flow structures of bionic cylinders based on harbor seal vibrissa. *Exp. Therm. Fluid Sci.* **99**, 169–180. (doi:10.1016/j.expthermflusci.2018.07.033)
47. Kim HJ, Yoon HS. 2018 Reynolds number effect on the fluid flow and heat transfer around a harbor seal vibrissa shaped cylinder. *Int. J. Heat Mass Transf.* **126**, 618–638. (doi:10.1016/j.ijheatmasstransfer.2018.05.083)
48. Morrison HE, Brede M, Dehnhardt G, Leder A. 2016 Simulating the flow and trail following capabilities of harbour seal vibrissae with the lattice Boltzmann method. *J. Comput. Sci.* **17**, 394–402. (doi:10.1016/j.jocs.2016.04.004)
49. Liu G, Xue Q, Zheng X. 2019 Phase-difference on seal whisker surface induces hairpin vortices in the wake to suppress force oscillation. *Bioinspir. Biomim.* **14**, 66001. (doi:10.1088/1748-3190/ab34fe)
50. Lyons K, Murphy CT, Franck JA. 2020 Flow over seal whiskers: importance of geometric features for force and frequency response. *PLoS ONE* **15**, e0241142. (doi:10.1371/journal.pone.0241142)
51. Gläser N, Wieskotten S, Otter C, Dehnhardt G, Hanke W. 2011 Hydrodynamic trail following in a California sea lion (*Zalophus californianus*). *J. Comp. Physiol. A Neuroethol. Sensory Neural Behav. Physiol.* **197**, 141–151. (doi:10.1007/s00359-010-0594-5)
52. Dehnhardt G, Mauck B. 2008 Mechanoreception in secondarily aquatic vertebrates. In *Sensory evolution on the threshold : adaptations in secondarily aquatic vertebrates* (eds JGMH Thewissen, S Nummela), pp. 295–314. Berkeley, CA: University of California Press.
53. Murphy CT, Reichmuth C, Eberhardt WC, Calhoun BH, Mann DA. 2017 Seal whiskers vibrate over broad frequencies during hydrodynamic tracking. *Sci. Rep.* **7**, 1–6. (doi:10.1038/s41598-017-07676-w)
54. Muthuramalingam M, Bruecker C. 2019 Seal and sea lion whiskers detect slips of vortices similar as rats sense textures. *Sci. Rep.* **9**, 1–15. (doi:10.1038/s41598-019-49243-5)
55. Hover FS, Triantafyllou MS. 2001 Galloping response of a cylinder with upstream wake interference. *J. Fluids Struct.* **15**, 503–512. (doi:10.1006/jfls.2000.0364)
56. Wolfe J, Hill DN, Pahlavan S, Drew PJ, Kleinfeld D, Feldman DE. 2008 Texture coding in the rat whisker system: slip-stick versus differential resonance. *PLoS Biol.* **6**, 1661–1677. (doi:10.1371/journal.pbio.0060215)
57. van Netten SM. 2006 Hydrodynamic detection by cupulae in a lateral line canal: functional relations between physics and physiology. *Biol. Cybern.* **94**, 67–85. (doi:10.1007/s00422-005-0032-x)
58. Goulet J, Engelmann J, Chagnaud BP, Franosch JMP, Suttner MD, Van Hemmen JL. 2008 Object localization through the lateral line system of fish: theory and experiment. *J. Comp. Physiol. A* **194**, 1–17. (doi:10.1007/s00359-007-0275-1)
59. Diamond ME, Von Heimendahl M, Knutsen PM, Kleinfeld D, Ahissar E. 2008 'Where' and 'what' in the whisker sensorimotor system. *Nat. Rev. Neurosci.* **9**, 601–612. (doi:10.1038/nrn2411)
60. Neimark MA, Andermann ML, Hopfield JJ, Moore CI. 2003 Vibrissa resonance as a transduction mechanism for tactile encoding. *J. Neurosci.* **23**, 6499 LP–6496509. (doi:10.1523/JNEUROSCI.23-16-06499.2003)
61. Dougill G, Starostin EL, Milne AO, van der Heijden GHM, Goss VGA, Grant RA. 2020 Ecomorphology reveals Euler spiral of mammalian whiskers. *J. Morphol.* **281**, 1271–1279. (doi:10.1002/jmor.21246)
62. Ginter CC, Fish FE, Marshall CD. 2010 Morphological analysis of the bumpy profile of phocid vibrissae. *Mar. Mammal. Sci.* **26**, 733–743. (doi:10.1111/j.1748-7692.2009.00365.x)
63. Rinehart A, Shyam V, Zhang W. 2017 Characterization of seal whisker morphology: implications for whisker-inspired flow control applications. *Bioinspir. Biomim.* **12**, 066005. (doi:10.1088/1748-3190/aa8885)
64. Shatz LF, de Groot T. 2013 The frequency response of the vibrissae of harp seal, *Pagophilus groenlandicus*, to sound in air and water. *PLoS ONE* **8**, 1–12. (doi:10.1371/journal.pone.0054876)
65. Hans H, Miao JM, Triantafyllou MS. 2014 Mechanical characteristics of harbor seal (*Phoca vitulina*) vibrissae under different circumstances and their implications on its sensing methodology. *Bioinspir. Biomim.* **9**, 036013. (doi:10.1088/1748-3182/9/3/036013)
66. Quist BW, Faruqi RA, Hartmann MJZ. 2011 Variation in Young's modulus along the length of a rat vibrissa. *J. Biomech.* **44**, 2775–2781. (doi:10.1016/j.jbiomech.2011.08.027)
67. Ginter-Summarell CC, Ingole S, Fish FE, Marshall CD. 2015 Comparative analysis of the flexural stiffness of pinniped vibrissae. *PLoS ONE* **10**, 1–15. (doi:10.1371/journal.pone.0127941)
68. Young WC, Budynas R. 2001 *Roark's formulas for stress and strain*, 7th edn. New York, NY: McGraw-Hill Professional Publishing.
69. Hartmann MJ, Johnson NJ, Towal RB, Assad C. 2003 Mechanical characteristics of rat vibrissae: resonant frequencies and damping in isolated whiskers and in the awake behaving animal. *J. Neurosci.* **23**,

6510–6519. (doi:10.1523/JNEUROSCI.23-16-06510.2003)

70. Belli HM, Yang AET, Bresee CS, Hartmann MJZ. 2016 Variations in vibrissal geometry across the rat mystacial pad: base diameter, medulla, and taper. *J. Neurophysiol.* **117**, 1807–1820. (doi:10.1152/jn.00054.2016)
71. Beem H, Hildner M, Triantafyllou M. 2013 Calibration and validation of a harbor seal whisker-inspired flow sensor. *Smart Mater. Struct.* **22**, 014012. (doi:10.1088/0964-1726/22/1/014012)
72. Gul JZ, Su KY, Choi KH. 2018 Fully 3D printed multi-material soft bio-inspired whisker sensor for underwater-induced vortex detection. *Soft Robot.* **5**, 122–132. (doi:10.1089/soro.2016.0069)
73. Stocking JB, Eberhardt WC, Shakhsheer YA, Calhoun BH, Paulus JR, Appleby M. 2010 A capacitance-based whisker-like artificial sensor for fluid motion sensing. In *Proc. SENSORS, Waikoloa, HI, 1–4 November 2010*, pp. 2224–2229. New York, NY: IEEE.
74. Eberhardt WC, Shakhsheer YA, Calhoun BH, Paulus JR, Appleby M. 2011 A bio-inspired artificial whisker for fluid motion sensing with increased sensitivity and reliability. In *Proc. SENSORS, Limerick, Ireland, 28–31 October 2011*, pp. 982–985. New York, NY: IEEE.
75. Kottapalli AGP, Asadnia M, Hans H, Miao JM, Triantafyllou MS. 2014 Harbor seal inspired MEMS artificial micro-whisker sensor. In *Proc. 27th IEEE Int. Conf. on Micro Electro Mechanical Systems (MEMS), San Francisco, CA, 26–30 January 2014*, pp. 741–744. New York, NY: IEEE.
76. Kottapalli AGP, Asadnia M, Miao JM, Triantafyllou MS. 2015 Harbor seal whisker inspired flow sensors to reduce vortex-induced vibrations. In *Proc. 28th IEEE Int. Conf. on Micro Electro Mechanical Systems (MEMS), Estoril, Portugal, 18–22 January 2015*, pp. 889–892. New York, NY: IEEE.
77. Zhu L, Zeng L, Chen X, Luo X, Li X. 2015 A bioinspired touching sensor for amphibious mobile robots. *Adv. Robot.* **29**, 1437–1452. (doi:10.1080/01691864.2015.1069210)
78. Subramaniam V, Alvarado PVy, Weymouth G. 2017 Sensing on robots inspired by nature. In *Biomimetic microsensors inspired by marine life* (eds AGP Kottapalli, M Asadnia, J Miao, MS Triantafyllou), pp. 77–110. Cham, Switzerland: Springer International Publishing.
79. Alvarado PV, Subramaniam V, Triantafyllou M. 2013 Performance analysis and characterization of bio-inspired whisker sensors for underwater applications. In *Proc. 2013 IEEE/RSJ Int. Conf. on Intelligent Robots and Systems, Tokyo, Japan, 3–7 November 2013*, pp. 5956–5961. New York, NY: IEEE.
80. Eberhardt WC, Wakefield BF, Murphy CT, Casey C, Shakhsheer Y, Calhoun BH, Reichmuth C. 2016 Development of an artificial sensor for hydrodynamic detection inspired by a seal's whisker array. *Bioinspir. Biomim.* **11**, 56011. (doi:10.1088/1748-3190/11/5/056011)
81. Alvarado PVy, Subramaniam V, Triantafyllou M. 2012 Design of a bio-inspired whisker sensor for underwater applications. In *Proc. SENSORS, Taipei, Taiwan, 28–31 October 2012*, pp. 1–4. New York, NY: IEEE.
82. Fries F, Alvarado PVy. 2017 Whisker-like sensors with soft resistive follicles. In *Proc. 2017 IEEE Int. Conf. on Robotics and Biomimetics (ROBIO), Macau, Macao, 5–8 December 2017*, pp. 2038–2043. New York, NY: IEEE.
83. Kamat AM, Pei Y, Kottapalli AGP. 2019 Bioinspired cilia sensors with graphene sensing elements fabricated using 3D printing and casting. *Nanomaterials* **9**, 954. (doi:10.3390/nano9070954)
84. Kamat AM, Zheng X, Jayawardhana B, Kottapalli AGP. 2021 Bioinspired PDMS-graphene cantilever flow sensors using 3D printing and replica moulding. *Nanotechnology* **32**, 095501. (doi:10.1088/1361-6528/abcc96)
85. Kaidarova A *et al.* 2019 Wearable multifunctional printed graphene sensors. *NPJ Flex. Electron.* **3**, 1–10. (doi:10.1038/s41528-019-0061-5)
86. Li T, Jayawardhana B, Kamat AM, Kottapalli AGP. 2021 Source-seeking control of unicycle robots with 3-D-printed flexible piezoresistive sensors. *IEEE Trans. Robot.* (doi:10.1109/TRO.2021.3076964)
87. 2018 Seals' whiskers provide a model for the latest submarine detectors. *The Economist.* See https://www.economist.com/science-and-technology/2018/08/09/seals-whiskers-provide-a-model-for-the-latest-submarine-detectors.
88. Beem H. 2016 Seal whiskers inspire marine technology. *Ocean. Mag.* **51**, 82–85.
89. Shyam V, Ameri A, Poinsatte P, Thurman D, Wroblewski A, Snyder C. 2015 Application of pinniped vibrissae to aeropropulsion. In *ASME Turbo Expo 2015: Turbine Technical Conf. and Exposition*, pp. GT2015-43055, V02AT38A023. Montreal, Canada: ASME.
90. Sengupta D, Chen S-H, Michael A, Kwok CY, Lim S, Pei Y, Kottapalli AGP. 2020 Single and bundled carbon nanofibers as ultralightweight and flexible piezoresistive sensors. *NPJ Flex. Electron.* **4**, 9. (doi:10.1038/s41528-020-0072-2)
91. Sengupta D, Chen S-H, Kottapalli AGP. 2019 Nature-inspired self-powered sensors and energy harvesters. In *Self-powered and soft polymer MEMS/NEMS devices*, pp. 61–81. Cham, Switzerland: Springer International Publishing.
92. Hires SA, Pammer L, Svoboda K, Golomb D. 2013 Tapered whiskers are required for active tactile sensation. *Elife* **2**, 1–19. (doi:10.7554/elife.01350)
93. Huet LA, Rudnicki JW, Hartmann MJZ. 2017 Tactile sensing with whiskers of various shapes: determining the three-dimensional location of object contact based on mechanical signals at the whisker base. *Soft Robot.* **4**, 88–102. (doi:10.1089/soro.2016.0028)
94. Williams CM, Kramer EM. 2010 The advantages of a tapered whisker. *PLoS ONE* **5**, e8806. (doi:10.1371/journal.pone.0008806)
95. Asadnia M, Kottapalli AGP, Haghighi R, Cloitre A, Alvarado PVy, Miao J, Triantafyllou M. 2015 MEMS sensors for assessing flow-related control of an underwater biomimetic robotic stingray. *Bioinspir. Biomim.* **10**, 36008. (doi:10.1088/1748-3190/10/3/036008)
96. Zheng X, Wang W, Xiong M, Xie G. 2020 Online state estimation of a fin-actuated underwater robot using artificial lateral line system. *IEEE Trans. Robot.* **36**, 472–487. (doi:10.1109/TRO.2019.2956343)
97. Salumäe T, Kruusmaa M. 2013 Flow-relative control of an underwater robot. *Proc. R. Soc. A* **469**, 20120671. (doi:10.1098/rspa.2012.0671)